CHEMSUSCHEM

DOI: 10.1002/cssc.201100177

Carbon Nanotube Mass Production: Principles and Processes

Qiang Zhang, Jia-Qi Huang, Meng-Qiang Zhao, Wei-Zhong Qian, and Fei Wei*[a]

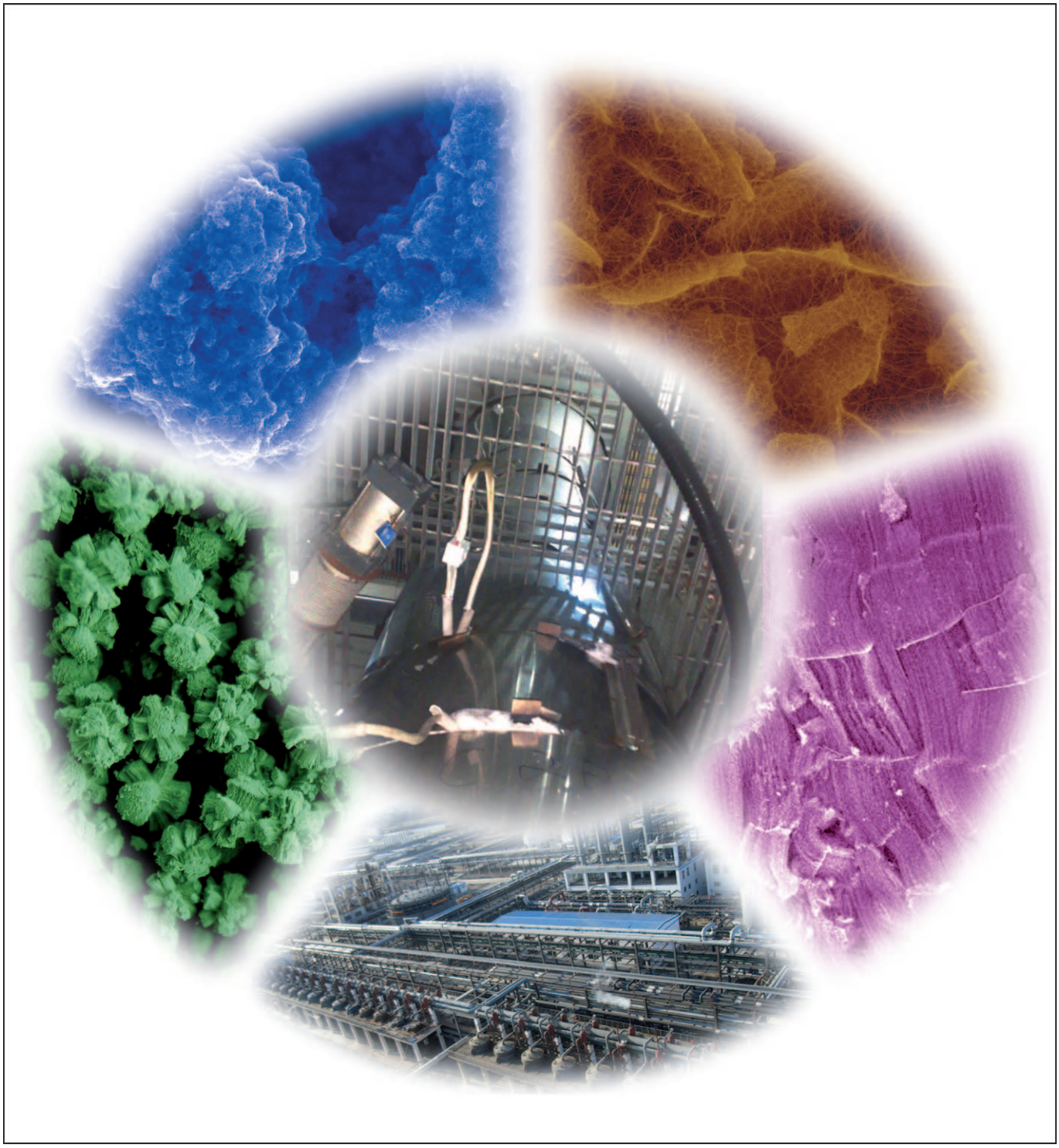

Our society requires new materials for a sustainable future, and carbon nanotubes (CNTs) are among the most important advanced materials. This Review describes the state-of-the-art of CNT synthesis, with a focus on their mass-production in industry. At the nanoscale, the production of CNTs involves the self-assembly of carbon atoms into a one-dimensional tubular structure. We describe how this synthesis can be achieved on the macroscopic scale in processes akin to the continuous tonne-scale mass production of chemical products in the modern chemical industry. Our overview includes discussions on processing methods for high-purity CNTs, and the handling of heat and mass transfer problems. Manufacturing strategies for agglomerated and aligned single-/multiwalled CNTs are used as examples of the engineering science of CNT production, which includes an understanding of their growth mechanism, agglomeration mechanism, reactor design, and process intensification. We aim to provide guidelines for the production and commercialization of CNTs. Although CNTs can now be produced on the tonne scale, knowledge of the growth mechanism at the atomic scale, the relationship between CNT structure and application, and scale-up of the production of CNTs with specific chirality are still inadequate. A multidisciplinary approach is a prerequisite for the sustainable development of the CNT industry.

1. Introduction

Carbon is one of the most important elements. Different shapes of elemental carbon have played important roles in humanity. Charcoal and soot have been known and utilized for various purposes since ca. 5000 BC, but as recently as 35 years ago only graphite and diamond were listed as carbon allotropes in textbooks. Since then, research on carbon has found fullerene, nanotubes, and graphene as new carbon allotropes (Figure 1 a–c). Although tubular nanocarbon forms (carbon filaments) were previously observed by Radushkevich and Lukyanovich in 1952, and Oberlin and Endo in 1976,[1] a 1991 paper by Iijima aroused worldwide interest in carbon nanotubes (CNTs).[2] A single-walled CNT (SWCNT) is a cylinder formed by wrapping a single-layer graphene sheet, while a multiwalled CNT (MWCNT) comprises an array of such nanotubes that are concentrically nested, like the rings of a tree's trunk. CNTs possess extremely high tensile strengths, high moduli, large aspect ratios, low densities, good chemical and environmental stabilities, and high thermal and electrical conductivities. They are a new type of high-performance carbon nanomaterial and in demand for various applications, including both large-volume applications (e.g., as components in conductive, electromagnetic, microwave absorbing, high-strength composites, battery electronic additives, supercapacitors or battery electrodes, fuel cell catalysts, transparent conducting films, field-emission displays, and photovoltaic devices) and limited-volume applications (e.g., as scanning probe tips, drug delivery systems, electronic devices, thermal management systems, and biosensors).[3] As a novel advanced functional material, CNTs have been considered for use in energy-saving chemistry, green catalytic processes, and advanced energy conversion and storage materials, and so have caught the attention of multidisciplinary scientists for use in developing a sustainable society. The number of articles on CNTs indexed by ISI Web of Science has continually risen in the past years (Figure 1 d). The total number of journal articles is still growing. However, the number of articles related to CNT synthesis began to decrease in 2009, while the number of application-related articles is still increasing, especially for applications in catalysis, energy, and environmental areas. Recently, CNTs have been used as fillers in advanced battery electronic additives, supercapacitors and battery electrodes, and lightweight high-strength composites at a scale of hundreds of tonnes. Other novel environmentally benign and resource-saving processes based on CNTs are being explored. The mass production of CNTs with a desired structure at a low cost is the first step in achieving these applications, and doing this production in a sustainable manner is a big challenge.

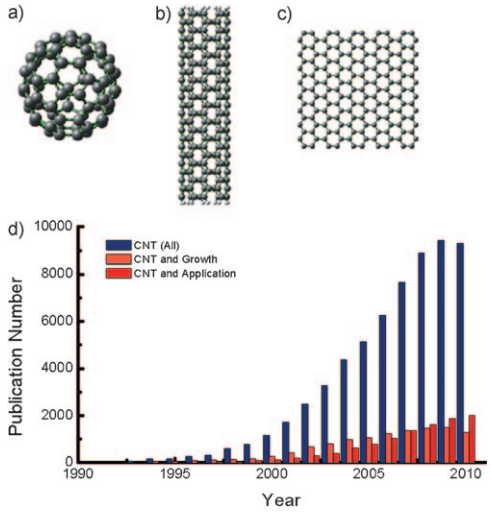

Figure 1. Illustrations of a) fullerene, b) a carbon nanotube, and c) graphene. (d) Number of publications on carbon nanotubes in ISI Web of Science on January 1, 2011.

Three main CNT synthesis methods have been developed: arc discharge, laser ablation, and chemical vapor deposition (CVD). A common feature of the arc discharge and laser ablation methods is high energy input by physical means, such as an arc discharge or a laser beam, to induce the assembly of

[a] *Dr. Q. Zhang, J.-Q. Huang, M.-Q. Zhao, Prof. W.-Z. Qian, Prof. F. Wei*
Beijing Key Laboratory of Green Chemical Reaction Engineering and Technology
Department of Chemical Engineering
Tsinghua University, Beijing (PR China)
Fax: (+86) 10-6277-2051
E-mail: wf-dce@tsinghua.edu.cn

carbon atoms into CNTs. This leads to a high degree of graphitization in the CNTs. However, these systems require vacuum conditions and continuous graphite target replacement, posing difficulties for continuous large-scale production. In CVD methods, the carbon source is deposited on a catalyst that causes it to decompose into carbon atoms, and tubular CNTs are formed at the catalyst site. The CVD process can be operated under mild conditions, for example, atmospheric pressure and moderate temperatures. The CNT structure, such as its diameter, length, and alignment, can be controlled well. Thus, CVD has the advantages of mild operating conditions, low costs, and controllable synthesis, and it is the most promising method for the mass production of CNTs. Various scalable CVD-based processes have been developed, including "Carbon Multiwall Nanotubes" of Hyperion Company,[4] the Endo process of Shinshu University,[5] the "CoMoCATProcess at SWeNT" of the University of Oklahoma,[6,7] the "HiPco Process" of Rice University,[8,9] the "Nano Agglomerate Fluidized" process of Tsinghua University,[10,11] the "Baytube" process of Bayer Company,[12] and processes for the supergrowth of SWCNT arrays[13–15] and super-aligned CNTs for yarn preparation,[16] as well as others. In 2006, a World Technology Evaluation Center study that focused on the manufacturing and applications of CNTs showed that there was MWCNT capacity of 300 tonnes per year and a SWCNT capacity of 7 tonnes per year in that year.[17] With more and more commercialized applications, the CNT industry appears to be on a path of growth.

The chemistry of CNT mass production can be summarized as carbon atoms assembling into a CNT structure. However, the structure and agglomeration of the produced CNTs are highly sensitive to the catalyst. Due to their high molecular weight (10^6–10^{13}), tubular structure, and complex physical and

Qiang Zhang graduated from the Chemical Engineering Department, Tsinghua University (PR China) in 2004. He continued doing research towards the mass production of CNTs at the same institute, and obtained his PhD in chemical engineering in 2009. After a short stay as a Research Associate at Case Western Reserve University (USA), he now holds a post-doctoral position at the Fritz Haber Institute of the Max Planck Society (Germany). His current research interests are nanocarbons, advanced functional materials, sustainable chemical engineering, and energy conversion and storage.

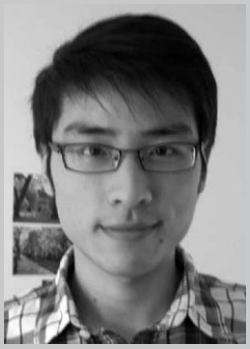

Meng-Qiang Zhao is currently a PhD candidate at the Department of Chemical Engineering, Tsinghua University (PR China). He is presently a one-year visiting scholar at University of Virginia (USA). His research interests are synthesis chemistry, mass production, assembly of CNTs and lamellar particles, and applications in heat management and packages.

Wei-Zhong Qian obtained his PhD in chemical engineering from Tsinghua University (PR China) in 2002. He was appointed an assistant professor in 2002 and associate professor of chemical engineering of Tsinghua University in 2005. His scientific interests are nanomaterials, advanced catalysis, and chemical engineering.

Jia-Qi Huang graduated from the Chemical Engineering Department, Tsinghua University (PR China) in 2007, and is currently a PhD candidate there. He is at present a visiting student in Prof. P. M. Ajayan's group (Rice University, USA). His research interests are the design of catalysts, mass production of CNTs/graphenes, process intensification, the applications of CNTs/graphenes in multifunctional composites, and energy conversion and storage. He was awarded the Education Ministry Academic Award for Talented PhD Candidates.

Fei Wei obtained his PhD in chemical engineering from China University of Petroleum in 1990. After a postdoctoral fellowship at Tsinghua University (PR China), he was appointed an associate professor in 1992 and professor of chemical engineering of Tsinghua University in 1996. His scientific interests are technological applications of chemical reaction engineering, multiphase flow, advanced materials, and sustainable energy. He has authored and co-authored over 200 refereed publications. He was awarded the Young Particuology Research Award for his contributions in the field of powder technology.

chemical properties, the continuous mass production of CNTs is a big challenge. In fact, the mass production of CNTs is a very complex process with diverse time and length scales. On the microscopic scale, it is a process in which carbon atoms self-assemble into a one-dimensional tubular structure (chemistry of CNT synthesis). On the macroscopic scale, it is the continuous mass production of a chemical product on the ton scale that is akin to those of the modern chemical industry, and includes processing, for high-purity MWCNTs and SWCNTs, and heat and mass transfer processes (chemical engineering of CNT production). Although extensive researches on the basic behavior of CNT growth have been performed, much of these works were conducted under ideal conditions, far from those used in industry. For example, the growth of CNTs is commonly investigated in a small laboratory reactor capable only of milligram or gram scale, in which the heat and mass transfer during the CNT growth are not severe problems, and the small amount of catalyst avoids the strong stress on the powder that can affect the growth behavior. However, when CNTs are grown on the ton scale in an industrial reactor, engineering science at the atomic scale, nanoscale, mesoscale, reactor scale, plant scale, and ecological scale all have to be taken into consideration to achieve a safe process for efficient mass production. The engineering science and chemistry of CNT synthesis are the basis to realize the goal of CNT mass production. It is hoped that this Review on the mass production of CNTs from the viewpoint of academia, especially on the engineering science, will be useful for the sustainable growth of the CNT industry.

CNT research has been a hot topic during the past 20 years, and much progress has been made. There are numerous Reviews that cover the synthesis, properties, and applications of SWCNTs,[18,19] MWCNTs,[18,20,21] and aligned CNTs.[22] This Review highlights the works and achievements on the mass production of CNTs in the last 20 years. We focus on the state-of-the-art mass production technology for various kinds of CNTs and the engineering science of CNT production. In the second part, the synthesis route to CNTs is illustrated to give the basic chemistry for their mass production. The engineering principle of scale up and mass production is discussed using a multi-scale space-time analysis. Current challenges and future strategies are discussed. Some other important issues in CNT production, such as their purification, properties, and applications, are only briefly considered in this Review.

2. State-of-the-Art of Carbon Nanotube Synthesis Principles

In the history of materials science, controllable synthesis has been a limiting factor in the adoption of new materials, and it was usually a breakthrough in the synthesis route that paved the way for their wide use. In this respect, the history of CNTs has been no exception. In the early years after their discovery, researches on CNTs were mainly theoretical and microscopic characterization works because of their limited availability. It was only after the development of techniques for the controllable synthesis of CNTs by arc discharge, laser ablation, and CVD that more researchers had access to more samples, which promoted the exploration of the fascinating science and technology of CNTs. Due to this progress, CNTs with controllable structure and alignment have now been widely investigated. Many applications require CNTs with very specific structures and agglomeration states. Conventionally, CNTs are classified into SWCNTs and MWCNTs by the number of walls. According to their agglomeration behavior, CNTs can be divided into two kinds: aggregates in which the CNTs are randomly entangled (Figure 2a and b), and arrays in which the CNTs are nearly parallel to each other (Figure 2c and d). According to the relationship between the growth direction of the CNTs and the substrate, there are vertically aligned CNTs (VACNTs; Figure 2c) and horizontally aligned CNTs (HACNTs; Figure 2d). This means that during CNT synthesis, both the atomic-scale synthesis of S-/MWCNTs and the mesoscale CNT organization should be considered. This Review will consider the state-of-the-art of CNT synthesis in this way. The growth manner and catalyst design are quite different for agglomerated CNTs and V-/HACNTs. The former is reviewed first.

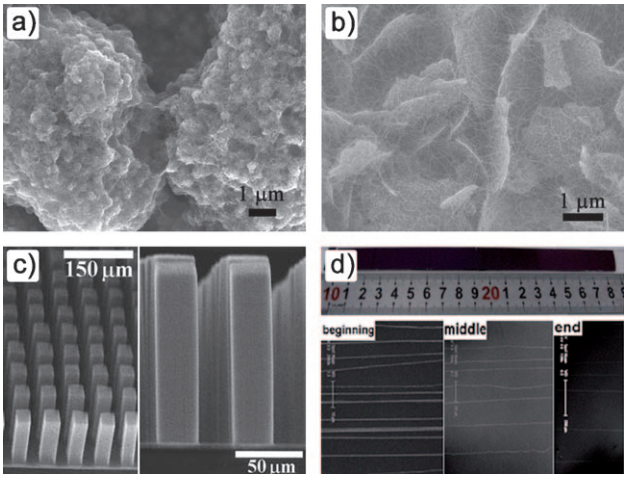

Figure 2. Agglomeration behavior of CNTs. a) MWCNTs (Reproduced with permission from Ref. [21]. Copyright 2008 Elsevier.) b) SWCNTs,[23] c) Vertically aligned MWCNTs (Reproduced with permission from Ref. [24]. Copyright 1999 American Association for the Advancement of Science.), and d) horizontally aligned SWCNTs (Reproduced with permission from Ref. [25]. Copyright 2009 American Chemicals Society).

2.1. Agglomerated CNTs

2.1.1. Agglomerated MWCNTs

In 1991, Iijima reported MWCNTs in carbon soot obtained by an arc discharge method.[2] One year later, Ebbesen and Ajayan demonstrated the growth and purification of MWCNTs at the gram level by an improved arc discharge method.[26] The laser ablation technique for CNT synthesis was developed in 1995.[27] The CVD of hydrocarbon gases has been used to make carbon fibers, carbon filaments, and nanotube materials for more than 20 years. In fact, carbon filaments were produced by passing cyanogen over red-hot porcelain in 1890.[28] The formation of

carbon filaments on metal catalysts is one of the main reasons for coke formation in many industrial processes (e.g., stream cracking, dehydrogenation, aromatization, catalytic reforming). MWCNTs are also one kind of coke, however, research work in the past century mainly focused on effective ways to reduce coke formation.[29] During this time, some pioneering researches were carried out to understand the formation mechanism and controllable synthesis of nanocarbons on metal catalysts.[30] In the 1980s, Endo et al. developed a floating catalyst reactor that used catalyst particles of 10 nm diameter for carbon nanofiber/MWCNT growth.[5] Hyperion Company had applied for a patent for CVD synthesis of 3~75 nm "carbon fibers," comprising multilayer graphite sheets wrapped into coaxial cylindrical tubes, in 1984.[4] The "carbon fibers" should be named MWCNTs. After Iijima's landmark paper, the first report on CVD growth of MWCNTs (carbon microtubules with the fullerene structure) by catalytic decomposition of C_2H_2 over Fe particles on graphite at 700 °C came from Jose-Yacaman et al. in 1993.[31] Subsequently, several growth systems for high-yield growth of MWCNTs have been developed. Selected important catalyst systems for the high-yield growth of MWCNTs are presented in Table 1, by time sequence.

Table 1. Selected results of agglomerated MWCNT growth.

Method[a]	Catalyst	*T* [°C]	Diameter [nm]	Yield	Ref.
AD	–	3000	2–20	/	[26]
CVD	Fe/graphite	700	5–50	/	[31]
CVD	Fe/SiO_2	500–800	15–20	/	[32]
LA	–	3000	5–20	/	[27]
CVD	Fe/SiO_2	650–800	10–20	30–116%	[33]
CVD	Ni/MgO	600	15–20	166–480%	[34]
CVD	$Co/Mo/Al_2O_3$	700	5–25	2–25%	[35]
FBCVD	Fe/Al_2O_3	500–700	10–40	1–20	[11]
CVD	Co/Mo/MgO	1000	0.5–3.0	16%	[36]
FBCVD	Fe/SiO_2	550–1050	10–20	10–50%	[37]
CVD	Ni/Mo/MgO	1000	9–20	10–100%	[38]
CVD	Co/Al-LDH	700	10–50	188%	[39]
FBCVD	Fe/Al_2O_3	550–750	8–21	10-70%	[40]
FCVD	ferrocene	830	20–70	/	[41]
CVD	$Co/Mo/Al_2O_3$	700	5–15	280–480%	[42]
FBCVD	$Fe/Co/CaCO_3$	600–850	10–20	1100%	[43]
CVD	$Ni/Fe/Al_2O_3$	600	19–45	6000%	[44]
CVD	Ni/SiO_2	680	15–40	124–426%	[45]
FBCVD	Fe/Mo/MgO	600–1000	5–60	66–400%	[46]
FCVD	Ferrocene	600–1000	10–200	/	[47]
CVD	Mo/MgO	900	5–7	33.4%	[48]
CVD	$Fe/Co/Al_2O_3$	700	3–24	14–56%	[49]
FBCVD	$Fe(Ni)/Al_2O_3$	700–850	15–30	70–300%	[50]
CVD	Co/W/MgO	1000	1.2–10	4–47%	[51]
CVD	Ni/Mg/Al-LDH	700	30–50	109–254%	[52]
CVD	Co/Zn/Al-LDH	625	20–30	/	[53]
FBCVD	Ni/SiO_2	450–850	37–91	2–145%	[54]
CVD	$Fe/Mo/Al_2O_3$	800–1100	2–15	/	[55]
FBCVD	Ni/Al_2O_3	650–800	8–20	2–17%	[56]
FBCVD	$Fe/Mo/Al_2O_3$	850	1.4–4.2	274%	[57]
CVD	Ni/Mg/Al-LDH	550–750	10–30	/	[58]
CVD	Co/Al-LDH	850	20–60	560–625%	[59]
CVD	$Ni(OH)_2/Al$	400–600	5–35	/	[60]
CVD	Co/Mn/Zn/Al	650	7–30	17900%	[61]

[a] AD: arc-discharge; LA: laser ablation; FBCVD: fluidized-bed CVD.

The catalyst is the key factor for CNT growth in CVD methods. Transition metals, especially Fe, Co, and Ni, are active for CNT synthesis (Table 1). These active elements are usually loaded onto a catalyst support by co-precipitation or other loading methods widely used in petroleum and chemical processes. However, the CNTs grow on the catalysts, that is, they are deposited on the catalyst surface, which means the catalyst is not a "catalyst", since it is only used once. This is similar to the catalysts used for polymerization, which are consumed during the monomer polymerizing process and left in the polymer products. The volume of the catalyst/CNT system increases with CNT growth, which is an obvious and important difference from catalytic processes in petroleum and chemical processes. At the present time, CVD is the most-investigated method for CNT mass production due to its much higher yield and simpler equipment, as compared with arc discharge and laser ablation. CVD can be conducted in a wide range of growth temperatures, from 500 to 1200 °C (Table 1). This is a relatively moderate temperature range, which makes it possible to carry out CVD in different kinds of reactors including fixed-bed, moving bed, fluidized-bed, and others (Table 1). The development of better catalysts and reactors has resulted in dramatically improved yields of agglomerated MWCNTs from CVD methods over the years. However, agglomerated MWCNTs are difficult to disperse and their lengths cannot be properly controlled, which limits their applications to the fields of composite reinforcement and as electrodes or electrode fillers in energy conversion and storage devices.

2.1.2. Agglomerated SWCNTs

The first success in producing substantial amounts of SWCNTs with Fe as catalyst by arc discharge was achieved by Iijima and Ichihashi in 1993.[62] Meanwhile, Bethune et al. reported that with the addition of Co in the anodes, SWCNTs can also be obtained by the arc discharge method.[63] The SWCNTs grown by arc discharge had few defects, and showed good performance for transparent conductive film applications.[83] The growth of high quality SWCNTs at the 1–10 g scale was first achieved by Smalley and co-workers using a laser ablation (laser oven) method.[65] CVD is still the most cost-effective and convenient method for the controllable growth of SWCNTs. In the first reported use of this method, Dai et al. reported the generation of SWCNTs by thermolytic processes using Mo particles and CO (CO disproportionation) at 1200 °C.[64] In 1998, Cheng et al. demonstrated that SWCNT ropes can be obtained using the floating catalyst process with thiophene as a sulfur source together with ferrocene and benzene.[67] Sen et al. produced SWCNTs by the pyrolysis of $Fe(CO)_5$ in the presence of CO and benzene.[84] Dai et al. found that the use of methane as carbon feedstock and alumina-supported catalysts allowed the growth of high quality SWCNTs by CVD.[68] Liu et al. reported that a catalyst prepared by supercritical drying at high pressure and temperature showed high activity and selectivity for the growth of SWCNTs.[85] Smalley et al. reported a HiPco process for the high-yield growth of SWCNTs, in which the catalysts for SWCNT growth were formed in situ by thermal decomposition

of $Fe(CO)_5$ in a heated flow of CO at pressures of 1–10 atm and temperatures of 800–1200 °C.[9] Resasco et al. reported the controlled production of SWCNTs based on a family of Co-Mo catalysts, which has since been developed into the CoMoCat process for SWCNT production in a fluidized-bed reactor.[7,86] Our group selected Fe/MgO as the catalyst for SWCNT production because Fe/MgO is a stable and low-cost catalyst, and it can be easily removed by a relatively mild acid treatment.[78] A series of SWCNT growth systems have been developed. The details are given in Table 2.

Table 2. Selected results of agglomerated SWCNT growth.

Method[a]	Catalyst	*T* [°C]	Yield	Ref.
AD	Fe	~3000		[62]
AD	Co[b]	~3000		[63]
CVD	Mo	1200		[64]
LA	Ni-Co	~3000/1200		[65]
AD	NiY	~3000		[66]
FCVD	ferrocene	1100–1200		[67]
CVD	Fe_2O_3/Al_2O_3	1000		[68]
CVD	$Fe/Mo/Al_2O_3$	850	20–60%	[69]
CVD	$Fe(CO)_5$	1200	25–44%	[8,9]
CVD	Fe/Co/MgO	1000	5.5–7.6%	[70]
CVD	$Co/Mo/SiO_2$	600–800	0.33–1.8%	[6,7]
CVD	Fe/MgO	850	8–20%	[71]
CVD	Fe/Mo/MgO	800	550%	[72]
CVD	$Fe(Mo)Al_2O_3$	900	0.1–10%	[73]
CVD	Fe/Co/Y-zeolite	800		[74]
CVD	Ni/SiO_2	760		[75]
TCVD	$Mo/Fe/Al_2O_3/Si$	725–925		[76]
CVD	Fe/MgO	900		[77]
CVD	Fe/MgO	900	11%	[78]
CVD	Fe/Mg/Al-LDH	900		[79]
CVD	Fe/Mo/Al film	700–1000		[80]
CVD	Fe/MgO	900	5.2%	[81]
CVD	Fe/Mg/Al-LDH	900	17.6%	[23]
CVD	Co/Mg/Al-LDH	900		[82]
CVD	Ni/Mg/Al-LDH	900		[82]

[a] AD: arc discharge; LA: laser ablation; FCVD: floating catalyst CVD; TCVD: thermal CVD. [b] LDH: layered double hydroxide.

For the production of SWCNTs, the arc discharge and laser ablation methods can give high-quality SWCNTs with few defects because of their ultrahigh energy input. However, just like the production of MWCNTs, these two methods also suffer from the high demands on equipment and low yield of SWCNTs (often as the byproduct of carbon ash). CVD can be conducted at a relatively low temperature (though higher than that used for MWCNTs), and is therefore advantageous for the scaling up of SWCNT production. Fe metal nanoparticles are the most widely investigated catalyst for the mass production of SWCNTs. The key issue in the production process is to maintain the state of dispersion of the metal nanoparticles (diameter below 3 nm) during CVD growth. Methods have been proposed to prevent the migration and sintering of metal particles on the support to maintain the stable growth of SWCNTs, including using the strong metal–support interaction,[87] mesoporous supports,[74,88] precursor mediated reduction,[89] and others. It should be noted that the yield of SWCNTs is much lower than that of MWCNTs. This is partly due to the low graphite sheet number in SWCNTs, such that a single SWCNT is thousands of times lighter than a single MWCNT. Therefore, for the same density and length of CNTs, the yield of SWCNTs will always appear to be much lower. In addition, SWCNTs are more flexible than MWCNTs, and are more prone to get entangled into agglomerates, which then stop the growth.

2.2. Aligned CNTs

Compared to agglomerated CNTs, CNTs in aligned form possess several outstanding properties, such as uniform orientation, extra high purity, and easy spinnability into macroscopic fibers, and others. With the discovery of efficient catalysts and processes for agglomerated S-/MWCNT growth, many research groups shifted their attention to aligned CNTs. VACNTs are CNTs that are oriented vertically to the substrate, and they are produced with a high area density. They can be used for both large volume applications (e.g., field emission devices, anisotropic conductive material, permeable membrane, filtration membrane material) and limited-volume applications (e.g., nanobrushes, sensors, electronic devices). HACNTs are promising for limited-volume applications in the microelectronics industry. Due to the differences between the growth modes of vertically and horizontally aligned CNTs, the state-of-the-art of aligned CNT synthesis is divided into two sections.

There are two ways to get aligned CNTs. One way is to physically align CNTs after the growth of random CNT agglomerates. Various methods, including polymer slitting,[115] electric field, magnetic field and chemical bond assisted orientation,[116] and gas or liquid shearing,[117] have been used to align CNTs into arrays. However, these physical processes involve complex procedures. Therefore, the second method of direct synthesis of aligned CNTs has received more attention in recent years. For the accurate controlled growth and alignment of CNTs on a large scale, it is difficult to use arc discharge[118] and laser ablation methods, and CVD is the preferred method for the synthesis of aligned CNTs. The key factor in the growth is the preparation of the metal nanoparticle catalysts on substrates, including the way to prepare metal nanoparticle catalysts in situ in the floating catalyst process

2.2.1. Vertically aligned CNTs

A VACNT array was firstly synthesized in 1996 by restricting the CNT orientation by distributing catalyst nanoparticles in nanochannels.[90] The length of the VACNTs could reach 2 mm.[119] Other ordered templates, such as anodic aluminum oxide (AAO) and zeolites, can also be used as the substrates for VACNT array growth.[99,120] If the catalyst is properly deposited on a flat substrate, a VACNT array can also be obtained through thermal CVD.[24,91,92] A SWCNT array was synthesized on Si wafer with the assistance of water steam as an additive in 2004.[14] The existence of oxygen can also promote the growth of VACNTs in a similar process. The nanoparticles can also be directly dispersed on the substrate for VACNT

growth.[100] In a floating catalyst process, in which the catalyst precursors are fed into the reactor with the carbon source, the catalyst particles are formed in situ for VACNT array growth.[84,121] When the growth temperature is in the range of 600–900 °C and a flat substrate is used, VACNT arrays can be easily synthesized.[93] The floating catalyst CVD method requires relatively simple equipment, with no need for a vacuum system, and avoids the tedious procedure of catalyst preparation as well, leading to a lower cost. Long VACNT arrays can be easily obtained,[122] however, catalyst particle formation and CNT growth are strongly coupled, and the reaction behavior and transport phenomena are complicated in this process. A brief summary of the synthesis of VACNT arrays is given in Table 3.

Table 3. Selected results of vertically aligned CNT growth.

Method[a]	Catalyst	*T* [°C]	Diameter [nm]	Ref.
CVD	Fe/mesoporous SiO_2	700	~30	[90]
CVD	Co/SiO_2 plate	950	30–50	[91]
PECVD	Ni/glass	<666	~100	[92]
TCVD	Fe/porous Si	700	14–18	[24]
FCVD	ferrocene	675	20–25	[93]
FCVD	$FeC_{32}N_8H_{16}$	800–1100	~40	[94]
TCVD	Co/Ni/Si	800–900	~110	[95]
FCVD	ferrocene	1100	10–30	[96]
FCVD	ferrocene	800	30–50	[97]
FCVD	ferrocene	800	10-200	[98]
CVD	Co in AAO	500	~90	[99]
CVD	Co/Mo/quartz	800	1.0–2.0	[100]
TCVD	Fe/Al(Al_2O_3)/Si	750	1–3	[14]
FCVD	ferrocene	700–760	~27	[101]
PECVD	Al_2O_3/Fe/Al_2O_3/Si	600	0.7–3	[102]
TCVD	Fe/Al_2O_3/Si	750	8–15	[103]
FCVD	ferrocene	820	70–130	[104]
TCVD	Co/Mo/Si	750	0.8–2	[105]
TCVD	$CoCrPtO_x$/Si	600	3–3.5	[106]
TCVD	FeVO/Si	810–870	2–6	[107]
FCVD	ferrocene	850	30–50	[108]
PECVD	Fe/Al/SiO_2/Si	750	0.8–2	[109]
HFCVD	Fe/Mo/Al_2O_3/Si	600–750	0.7–8	[110]
CVD	Fe/Al_2O_3/Si	770	6–15	[111]
CVD	Fe/Al_2O_3/Si	750	10–30	[112]
FBCVD	Fe/Mo/vermiculite	650	5–12	[113]
TCVD	Co/Mo/quartz	800–900	1–8	[114]

[a] FCVD: floating catalyst CVD; TCVD: thermal CVD; HFCVD: hot-filament CVD; PECVD: plasma-enhanced CVD; FBCVD: fluidized-bed CVD.

VACNTs are commonly synthesized on a substrate that supports the growth and alignment of the CNTs. As shown in Table 3, the most common catalyst for VACNT synthesis is Fe. The nanoparticle size of the catalysts showed a clear correlation with the wall number of CNTs. The addition of promoters like Mo or an inert Al_2O_3 layer can greatly facilitate the dispersion and prevent sintering of the Fe nanoparticles. Individual CNTs in the arrays are considered to be of the same length as the VACNTs, which are often on the millimeter scale. Actually, the lengths of the CNTs would be more than the height of the array when the tortuous morphology of the CNTs is taken into consideration. For this type of synthesis, the metal catalyst distributed on the surface of the substrate can be used more efficiently and enough space is available for CNT growth, thus, the yield of VACNTs is much higher than that of agglomerated CNTs. Presently, investigations on the growth termination mechanism of ultra-long VACNTs, and the precise control of CNT structures, such as chirality, with a view towards applications in microelectronics and optics are intensely pursued in this area.

2.2.2. Horizontally aligned CNTs

The controllable synthesis and organization of CNTs into horizontally aligned arrays is a prerequisite for their large-scale integration into nanocircuits. The controlled deposition of preformed nanotubes from solution onto a substrate with well-defined structures mediated by substrate surface hydrophobic/hydrophilic properties,[123] electric and magnetic interaction,[124] and chemical bonding,[125] have been topics of intense research. To avoid solution contamination and ascertain the precise location of the HACNTs, the direct growth of HACNTs on a surface by CVD has been widely explored. Due to the horizontal growth mode of the CNTs (free of space resistance, especially for flow induced growth), superlong CNTs with lengths of up to 20 cm and a weight space velocity of $10^8\ g_{CNT}\,g_{cat}^{-1}\,h^{-1}$ have been achieved.

The key to get HACNTs onto a substrate surface is to apply a suitable aligning force to direct the growth of the nanotubes during CVD. A number of growth strategies have been developed for synthesizing HACNTs using various aligning forces, including electric-field-directed growth,[126] magnetic-field-directed growth,[156] gas-flow-directed growth,[129,157] and substrate-surface-oriented growth.[133,134] Among these, the gas-flow-directed growth, in which the feed gas is used to align the CNTs along the flow direction, using a fast heating CVD method is the most attractive.[129,157] A 'kite mechanism' was proposed, where a key component is that the CNTs grow above the substrate surface.[157] In this mechanism, during the 'fast heating' process, the convection of the gas flow between the substrate and feed gas lift the CNTs upwards and keep them floating and waving in the gas until they reach the laminar flow region, whereupon they descend onto the substrate. The growing CNTs float in the feed gas and grow along its flow direction.[157] Recently, ultralong SWCNT arrays were synthesized based on this approach. The growth of HACNTs can be directly obtained by well-defined crystal surfaces through lattice-directed epitaxy (by atomic rows), ledge-directed epitaxy (by atomic steps), and graphoepitaxy (by nanofacets). The formation of highly aligned, unidirectional, and dense arrays of long SWCNTs on a surface were first observed by CVD growth on a low quality C-plane sapphire. Details can be found in Table 4.

Similar to VACNT growth, flat substrates are also needed to support the growth of HACNTs. Compared to agglomerated CNTs and VACNTs, the volume density of HACNTs is much lower, and fewer entanglements occur, which help to maintain the growth of the CNTs that otherwise would be terminated. When CNTs are aligned into horizontal arrays, they hardly meet the space resistance that CNTs exert on one another in other

Table 4. Selected results of horizontally aligned CNT growth.

Method[a]	Catalyst	T [°C]	Substrate	Ref.
EFCVD	Fe	900	wafer	[126]
EFCVD	Fe	800	wafer	[127]
GCVD	Fe/Mo	900	wafer	[128, 129]
GCVD	$FeCl_3$	900	wafer	[130]
CVD	Fe	900	quartz	[131]
GCVD	FeMo	900	wafer	[132]
GECVD	ferritin	800	sapphire	[133]
GECVD	ferritin	900	sapphire	[134, 135]
GCVD	Co(Mo)	850	Si	[136]
MFCVD	Fe	750	SiO_2	[137]
GCVD[b]	$FeCl_3$	950	wafer	[138]
GECVD	ferritin	800	α-Al_2O_3	[139]
GCVD	Cu	925	wafer	[140]
GECVD	Fe(Mo)	900	sapphire	[141]
GCVD	$FeCl_3$, ferritin	900	wafer	[142]
GECVD	ferritin	900, 925	ST-cut quartz	[143]
GCVD	$FeCl_3/CoCl_2$	900–950	wafer	[144]
GECVD	Fe,Co,Ni	900	quartz	[145]
GCVD	Cu	900	ST-cut quartz	[146]
CVD	SWCNTs	975	wafer/quartz	[147]
GCVD	FeMo	950	wafer	[25]
GECVD	Cu	900	ST-cut quartz	[148]
CVD	SiO_2, Al_2O_3, TiO_2, Er_2O_3	900	wafer	[149]
GECVD	FeMo	900	SiO_2/Si wafer	[150]
GCVD[c]	$FeCl_3$	1000	SiO_2/Si wafer	[151]
GECVD	ferritin	750–900	ST-cut quartz	[152]
GECVD	Fe line	925	ST-cut quartz	[153]
GCVD	$DyCl_3$	900	SiO_2/Si wafer	[154]
GCVD[d]	$FeCl_3$	1000	SiO_2/Si wafer	[155]

[a] EFCVD: electrical-field-assisted CVD; MFCVD: magnetic-field-assisted CVD; GCVD: gas-flow-assisted CVD; GECVD: Graphoepitaxy CVD. If not specitfied, the CNT products were SWCNTs. [b] S/D/MWCNT. [c] TWCNT. [d] D/TWCNT.

growth modes, and they can easily extend their lengths. Thus, it is easy to control the length by controlling the growth time and substrate size. Moreover, the CNTs on the surface can be patterned with complex orientation to provide high-quality CNTs with a desired organization for applications in nanoelectronics and nanodevices. As the CNTs in HACNTs can be separately identified, it would also be an extraordinary platform to explore novel catalysts and growth mechanisms of CNTs. Recently, an advanced metal catalyst system was developed for the preferential growth of metallic or semiconductive CNTs on wafers. The CNTs distributed on a wafer can be easily transferred onto other substrates or TEM grids for structure observations and property tests. SWCNTs are commonly grown on substrates with a density of 0.03–45 tubes μm^{-1}. Not only SWCNTs, but also double- and tripled-walled CNTs were fabricated in this way.

2.3. Summary of CNT synthesis

After the twenty-year development of CNT synthesis, numerous works on the control of CNT structure and increasing synthesis efficiencies have been achieved. The chemistry of CNT growth has been comprehensively investigated, and catalytic CVD has been developed as the main approach for the controllable synthesis of CNTs with desired structures and patterns. Various transition metals, especially iron, have been shown to be efficient for CNT growth. Agglomerated CNTs with tunable wall number distributions, VACNTs with different patterns, and HACNTs with selected conductive properties have been produced. CNTs grown in an aligned way benefit from less interference with each other (less space resistance), better orientation, a higher CNT yield per metal catalyst, fewer structural defects, and longer lengths.

3. Engineering Principles of Carbon Nanotube Mass Production

The reports on CNT growth behavior provide us with the basic chemistry of CNT synthesis. However, this is not enough for the design of industrial reactors because of the strong coupling between the catalytic process and reactor heat/mass transfer in the mass production of CNTs. For example, in terms of the morphology, the CNT product cannot be considered as a uniform substance. Their momentum, heat, and mass transfer properties are obviously different from those of common fluids and powders, and pristine CNTs are very difficult to process. This Review describes how these problems are solved by the delicate control of the agglomerated structure of pristine CNTs. The agglomeration structure significantly affects the properties and applications of the CNTs. The CNT structure is grown in a bottom-up self assembly route, which is one discrete event. However, mass production is a continuous operation with macroscopic flow, reaction, and heat and mass transfer. For robust mass production, the CNT growth has to be considered not only at the atomic scale and as a macroscopic continuous operation, but also take into account the mesoscopic nanostructure and CNT architecture modulation, which are strongly coupled to both the atomic and macroscopic scales. Although this process resembles traditional chemical engineering processes and powder technology unit operations because the CNTs can be treated as a continuous fluid, there is also the need to consider the CNT structure. The gap between the microscopic and macroscopic scale needs further investigation. This is shown in the multiscale space-time analysis of the mass production of CNTs in Figure 3. The mass production process is considered on five scale levels:

1. CNT self-assembly at the atomic scale, including the growth conditions and growth mechanism of the CNTs, catalyst design, and controllable synthesis of individual CNTs. Many characteristics of the CNT products, including wall number, diameter, length, defects, chirality, crystallinity, and graphitization are determined at this scale.

2. As CNTs grow longer, various CNT agglomeration structures are formed due to the large aspect ratios and strong interactions between CNTs. These structures include agglomerated CNT particles, CNT arrays, suspended individual CNTs, and others. Actually, the agglomeration behavior of CNTs is the bridge between the atomic structure and their mass production. On the one hand, the interaction between CNTs causes stresses, which leads to the formation of CNTs with various agglomeration structures. On the other hand, different agglomer-

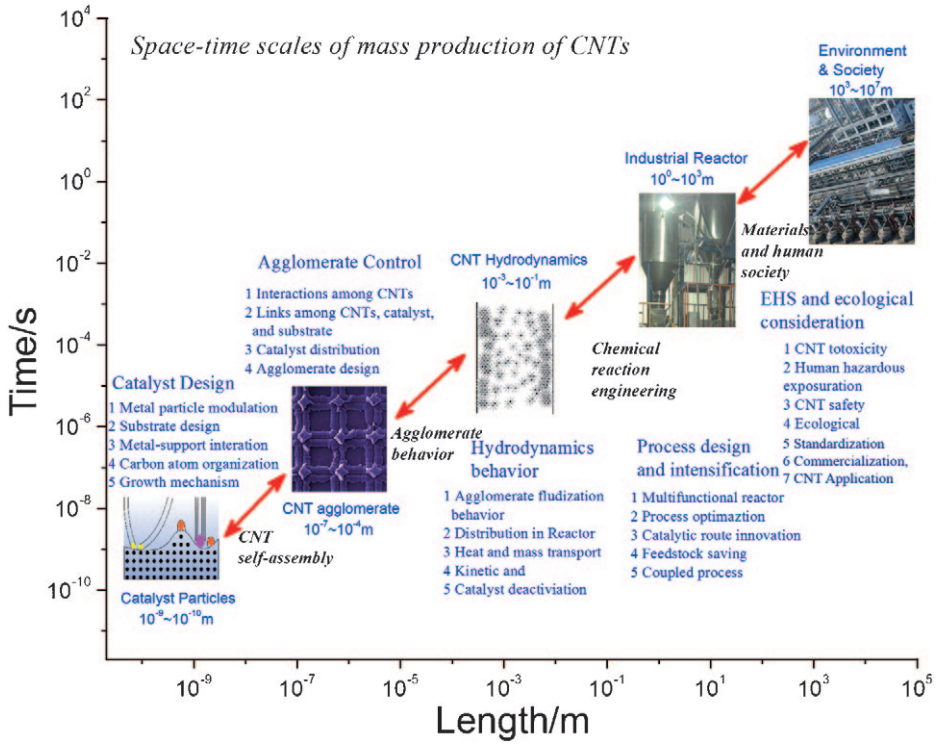

Figure 3. Multiscale space–time analysis of the mass production of CNTs.

safety, human health, and the long term influence on the biosphere have to be considered. Finding safe ways to use CNTs as advanced functional materials to improve our daily lives is a goal. This is an important step for the sustainable development of the CNT industry, and would need setting safety requirements for designing CNT structure and their efficient production process.

In the past twenty years, much engineering of CNT mass production have been carried out. The multiscale space-time analysis illustrated in Figure 3 is used here as a framework to classify these researches on CNT production into different scales according to their time-space scale. The detailed engineering science at the various scales is addressed.

ated states of CNTs have different hydrodynamic properties, heat and mass transfer rates, and catalyst deactivation behaviors, which determine the strategies for their mass production. The mesoscopic level is that in which the behavior of agglomerated nanostructure, including agglomerate morphologies, agglomeration mechanism, stress within agglomeration, and ways to control the agglomerates will be comprehensively reviewed to give the science and technology of agglomerated CNT and CNT array mass production.

3. The third scale is that of the transport phenomena and growth kinetics of CNTs, including the hydrodynamics, heat and mass transfer, apparent and intrinsic kinetics, and catalyst deactivation. CNTs can be randomly organized or aligned into specific agglomerates, similar to macromolecular polymers. However, CNTs have much higher molecular weights. Due to the unique transport properties and growth kinetics of CNTs and CNT agglomerates, traditional facilities have to be modified for CNT production. The modification of the hydrodynamic behavior of nanomaterials in the reactor is a basic problem and the key in reactor design and scaling up of this process.

4. Process intensification includes the use of better process operation that makes use of the relationship between the macroscopic operation and microscopic CNT structure, novel catalytic routes, and economical feedstocks or feeding methods. Macroscopic objects and various traditional chemical engineering concepts are involved at this level.

5. The fifth scale is that of environmental and ecological considerations, and the packing, delivery, application, standardization, and commercialization of CNTs. Exposure to CNTs will increase with their mass production and applications, and

3.1. Growth mechanism

Metal catalysts such as Fe, Co, and Ni show high activity for CNT growth (Tables 1–4). With these catalysts, hydrocarbons are readily decomposed on the surface of the transition metal, and surface/bulk diffusion of carbon atoms easily occurs on/in the metal catalyst. Recent breakthroughs on metal-catalyst-free growth of CNTs make non-metal residual CNT production feasible.[149,158] More advanced catalysts for commercialized CNT production are still needed.

The growth dynamics of nanocarbons on metal nanoparticles have been explored since the 1970s. Recent observations indicate that the metal catalysts are in the solid state.[159,160] Thus, the vapor-solid-solid (VSS) growth model derived from the vapor-liquid-solid (VLS) model for the growth of silicon whiskers,[161] is the one used for understanding the growth mechanism of CNTs. The dynamics of the catalyst state could be very complex, the surface of the catalyst is reconstructed, and there are fluctuations of the carbon concentration in the catalysts. The growth mechanism of CNTs is still not fully understood. Selecting the right materials and process parameters to synthesize CNTs with desired structures is still an art. In this section, new insights for CNT growth at an atomic scale are provided as a guide for diameter- and chirality-mediated CNT mass production.

3.1.1. Diameter-mediated CNT production

The diameter of the CNTs produced strongly depends on the size of catalyst nanoparticles. Small catalyst particles (0.5–5 nm) are efficient for SWCNT growth, and large catalyst parti-

cles (8–100 nm) are usually used as the catalyst for MWCNT growth. When discrete catalytic nanoparticles with diameters in the range of 1–2 and 3–5 nm were used for the growth of SWCNTs on substrates by CVD, SWCNTs with a diameter distribution of 0.9–2.7 and 1.5–6.0 nm were obtained, respectively.[162] A ratio between the catalyst particle sizes and CNT diameters close to 1.6 was also reported.[163] For supported Fe/MgO catalyst, with increasing content of Fe on the MgO support, both the diameter of the SWCNTs and the ratio of DWCNTs increased.[87] Zhang et al. found that S/D/MWCNTs were selectively synthesized when Fe/MgO catalysts with different Fe loadings (0.5–15 wt%) were used.[164] Zhao et al. reported a similar selectivity when Fe/Mg/Al LDHs were used as catalyst.[23] This was attributed to the small metal catalyst particles formed when the metal loading amount was low, and the dominating surface diffusion on the catalyst particles resulted in the selective formation of SWCNTs.[164,165] With increased metal loading amount, the metal atoms sintered into large nanoparticles. Both surface and bulk diffusion, which contribute to the outer and inner layer of DWCNTs, respectively, took place on a single catalyst particle. When the metal loading further increased, the sizes of the catalyst particles were in a large range of over 5 nm, and bulk diffusion of carbon dominated the growth of CNTs. Carbon atoms can accumulate at the surface of the catalyst and encapsulate the iron catalyst into the MWCNTs or produce carbon encapsulated metal particles, which depend on the precipitating rate of carbon from the catalyst.[23,164]

Though the size of catalyst particles shows strong relationship with the outer diameter of CNTs, the inner diameter of CNTs can vary strongly with the same catalyst particle size when introducing additives during the CNT growth. The inner diameter of MWCNTs is invariably in the range of 5–10 nm. By intentionally adding some alkali metal salts into the catalyst system, the inner diameter of the CNTs can be enlarged from 3–7 to 40–60 nm, while the outer diameter of about 60–80 nm is preserved.[166] Thin-walled CNTs can be formed by using chlorine-substituted benzene, $C_6H_{6-x}Cl_x$ ($x = 0$–3), as the carbon precursor. The ratio d_{in}/W, which is defined as the ratio of inner diameter and wall thickness of a nanotube, can be changed from 0.3 to 5.0.[167] This is because the additional Cl can bond with the dangling bonds of carbon or hydrogen atoms.[168] These factors disrupt the normal dissolution of carbon into the iron phase and the precipitation at the carbon/metal interface for small-inner-diameter CNTs.[167,169] It should be noted that the inner space of CNTs can provide a confined space for advanced catalysis, nanoreactors, and energy conversion/storage.[170] However, the precise control of the outer diameter, inner diameter, and number of walls of MWCNTs is still a big challenge.

3.1.2. Chirality-mediated CNT production

The structure (e.g., chirality and defect formation) of CNTs strongly depends on the dynamics of the catalyst particles during growth. Particular caps are favored by the epitaxial relationship with the solid catalyst surface and the corresponding tubes grow preferentially.[171] There is a minimum required metal cluster size to support SWCNT growth, and this cluster size can be used to control the diameter of the SWCNTs at temperatures relevant to CNT growth.[172] Strong electrostatic interactions, which are dominated by inner rather than frontier orbitals, are found between the cap rim atoms and the metal atoms they are in contact with.[173] To know the atom-by-atom growth of SWCNTs, in situ atomic characterization of CNT growth is needed.[159,160,174] Theoretical simulation is also a good way to get the atomic details of the growth of CNTs.[175] Recently, Ding et al. suggested that any nanotube can be viewed as a screw dislocation along the axis.[176] The kinetic mechanism and deduced predictions were remarkably confirmed by a broad base of experimental data.[177] The detailed steps show how adding a single C atom induces chirality change and how the incorporation of C_2 dimers leads to the growth of the tube.[178] The armchair and near-armchair CNTs are mostly produced when the growth mechanism is dominated by reactions such as C_2 addition to the cap rim atoms.[173] These ideas on CNT formation will enlighten the strategy for chirality control of manufactured CNTs.

However, experimental results also deviate strongly from theoretical predictions. Most as-grown CNTs are a mixture of metallic and semiconducting tubes. To meet the demands of the microelectronic industry for high-purity metallic or semiconducting CNTs, both post treatment and in situ growth have been explored. Density-gradient ultracentrifugation, a scalable technique, was developed to sort CNTs by diameter, bandgap, and electronic type.[179] Narrow-diameter distributions of SWCNTs (i.e., $>97\%$ within a 0.02 nm diameter range) can be obtained. Bulk quantities of S-/DWCNTs of predominantly a single electronic type can be produced by using competing mixtures of surfactants.[179,180] A series of surfactants/polymers have been used to separate SWCNTs with fixed chirality.[181] Novel SO_3 etching[182] and electrochemical etching[183] methods were also developed to obtain metallic or semiconducting CNTs. On the other hand, in situ growth methods are also good ways to obtain CNTs with certain chiralities. It was found that CVD on a Fe–Ru bimetallic catalyst[184] or a Cu–Fe/MgO catalyst procued by atomic layer deposition[185] produced predominantly (6,5) SWCNTs. Up to now, the production of CNTs with a desired chirality is still a big challenge for researchers.

3.2. Agglomeration mechanism

The growth mechanisms above are effective for controlling the CNT structure. However, the as-grown CNTs will cluster into agglomerated or aligned CNTs. The strategies for scale-up and mass production of CNTs strongly depend on the agglomeration process. In this section, the agglomeration behavior of CNTs is reviewed. To give a guideline for mass production, the scale-up methodology of agglomerated CNTs and aligned CNTs are also summarized.

3.2.1. Formation of CNT agglomerates

Agglomerated CNTs are three-dimensional network structures composed of large numbers of CNTs. They form very easily be-

cause CNTs are prone to entangle during growth on powder catalysts. Usually, the CNT catalyst is composed of nanoparticles, that is, a metal phase distributed on the catalyst support. With the introduction of a carbon source, CNTs will grow out from the particles. As shown in Figure 4, the morphology of the Fe/Mo/Al_2O_3 powder catalyst will change with the growth

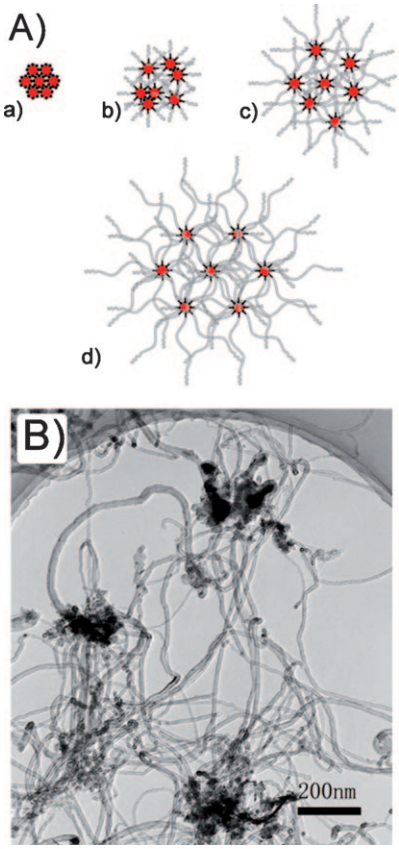

Figure 4. A) Mechanism of CNT agglomeration: a) an original catalyst particle; b) the catalyst particle structure is crushed by CNT growth; c) the catalytic sites are separated and sub-agglomerates form; d) fully developed agglomerates. B) Structure of a CNT agglomerate. (Reproduced with permission from Ref. [186]. Copyright 2003 Elsevier.)

of CNTs and the catalyst particles will be crushed. In the initial period, growing CNTs crush the catalyst particles into small clusters, forming separated catalytic sites.[186,187] With increasing carbon deposition, the catalysts will be crushed further and the CNTs will grow around the catalyst sites. The growing CNTs will push the crushed catalyst away and separate the sites from each other, leading to an increase in agglomerate size and a decreasing density as well (Figure 4c, d). The agglomerated structure and its evolution during CNT growth are of fundamental importance[188] for CNT mass production because a single CNT cannot be fluidized as it is a linear nanometer-scale material. The agglomeration, in which a three-dimensional network structure is developed that hydrodynamically behaves as a big particle, is the reason for the good fluidization behavior of agglomerated MWCNTs. If the catalyst structure is too strong to be crushed by the growing CNTs, the insides of the catalyst cannot be used for CNT synthesis and the yield will decrease severely. On the other hand, if the catalyst structure is too loose and easily broken the agglomerates will be crushed into small pieces and entrained out from the reactor.[21] When the agglomerated CNT product is kept moving in the reactor, the weak connection between the agglomerates is broken, which keeps the CNT material fluidizable. With a properly controlled agglomeration state, which gives a controlled fluidization state, MWCNTs can be efficiently produced in a fluidized bed reactor.

If the number of walls of the CNTs is decreased and they become double/single-walled, the CNTs obtained will be very flexible. The nucleation of CNTs can be considered as a self-assembly of carbon atoms into tubes after precipitation from a quasi-liquid saturated C-Fe solution. When S-/DWCNTs grow in a porous catalyst, as shown in Figure 5, regardless of whether

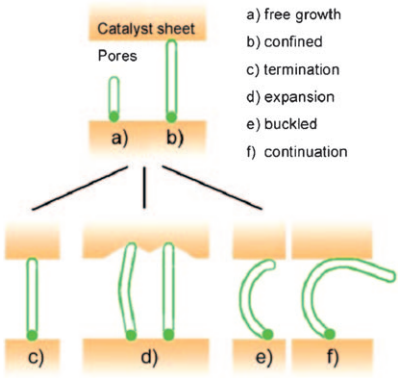

Figure 5. Confined growth of an individual CNT in a porous catalyst agglomerate: a) free growth, b) touching of the catalyst sheets, c) termination of the growth, d) pores of catalyst agglomerate broadened, e) buckling, and f) continued growth. (Reproduced with permission from Ref. [189]. Copyright 2008 Elsevier.)

in tip or root growth mode, the S-/DWCNTs all touch the catalyst sheet, and therefore three possible scenarios will occur: (1) if the catalyst agglomerate is strong and the CNTs cannot push apart to expand the catalyst agglomerate, growth will be terminated (Figure 5c); (2) if the strength of the porous catalyst is weak and the CNTs can expand the catalyst agglomerate, the CNTs will continue to grow (Figure 5d); (3) the CNTs cannot expand the catalyst agglomerate but can bend and buckle when the pore size is large enough, whereupon the CNTs can extend out from the pores of catalyst agglomerate and continue to grow (Figure 5e and f).[189] S-/DWCNT growth needs not only good dispersion of the active metal components on the catalyst support and a suitably large BET surface area, but also a proper catalyst structure. Any factor that can enlarge the pore size or reduce the strength of the catalyst (including the direct formation of large pores in a catalyst by a template, controlled critical drying of the catalyst,[85] minimizing catalyst support size,[190,191] aerosol catalyst,[67,192,193] or direct spray drying of the catalyst into very fine powders[194]) can provide a catalyst with a low bulk density and weak interaction in the agglomerates that will meet the requirements for

S/DWCNT growth in high yield, high purity and high quality. For instance, using an improved Fe/MgO catalyst with a larger sheet than the original catalyst and dominant pores larger than 180 nm, a mixture of DWCNTs and SWCNTs were obtained with high carbon yield and a high BET surface area of 1005 m^2g^{-1}, which was 1.5 times that of the CNTs grown on the original catalyst (~650 m^2g^{-1}).[189] Recently, Nie et al. reported that an ethanol-thermal treatment was effective for increasing the percentage of very large pores in the porous catalyst structure, and can be used for the growth of very high quality SWCNTs with much fewer defects.[81] Layered double hydroxides (LDH), also known as hydrotalcite-like materials, which are a class of two dimensional nanostructured anionic clays whose structure is based on brucite ($Mg(OH)_2$)-like layers, can be used as a novel catalyst for SWCNT growth with a huge BET surface area of 1289 m^2g^{-1}.[23] The LDH can form porous agglomerates, which is an ideal and efficient catalyst for SWCNT mass production in a fluidized bed reactor.[82]

3.2.2. Aligned CNT formation

The aligned CNTs were all obtained by a bottom-up self-assembly process during thermal/floating-catalyst CVD. The CNTs in the array grow simultaneously, and therefore the position of the growth site and the agglomeration mechanism of aligned structure formation are of much concern. To identify the growth sites of the CNTs in the vertically aligned array, various methods, such as isotope labeling by ^{13}C in the carbon source to detect the sequence of the formation of different CNT sections,[195] multi-layer growth with different growth times,[196–199] and catalyst labeling method[200] were used. For thermal CVD and floating catalyst CVD, the growth site of was indicated to be at the bottom of the VACNTs.[195–200] This mechanism gave the growth direction of isolated CNTs and informed us of the importance of maintaining the catalyst and carbon source at the bottom of the CNT arrays, but indicated little about the formation process of the array. To solve the basic question in aligned CNT formation to give an ordered self-assembled structure, especially when beginning from an initial random structure, Zhang et al. characterized the morphology of multi-layered CNT arrays and the change in the curvature of the CNTs (tortuosity) obtained by floating catalyst CVD (Figure 6 A). A Raman shift during growth was measured and used to characterize the presence of stress in the CNTs.[199] The synchronous growth of a CNT array induced by stresses among CNTs was found. This is shown in Figure 6. For VACNT growth, metal nanoparticles were deposited on the substrate first (Figure 6 B (a)), and the CNTs grew on these nanoparticles. At the beginning, the catalyst particles were in low density and the CNTs grew randomly on the substrate. At the same time, new catalyst particles formed and the CNTs grew longer (Figure 6 B (b)). When the CNTs exceeded a certain length, they get entangled with each other and formed a woven structure. Subsequently, new CNTs cannot grow freely on the surface due to the limited space in the horizontal and vertical directions: a compressive stress was placed on later formed curved CNTs and a tensile stress was placed on the weave-connected

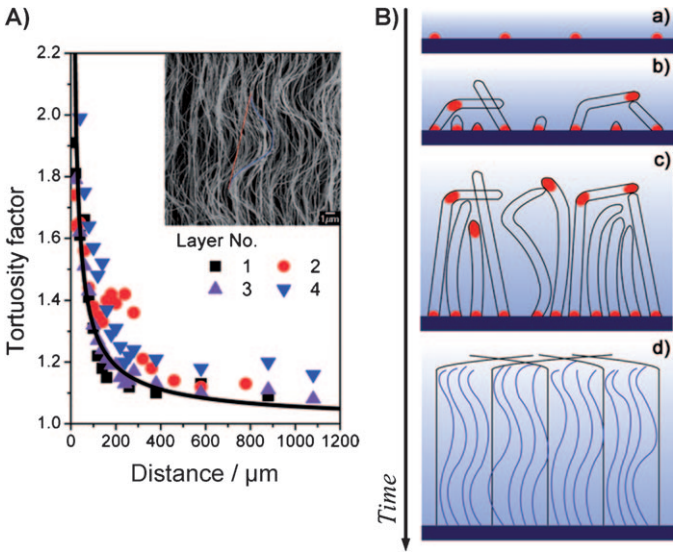

Figure 6. A) Tortuosity, defined as the length ratio of the blue to red lines in the inset to describe the curvature, was decreased from the top of CNTs. B) Schematic description of the synchronous growth of a CNT array with pristine stress in the heterogeneous catalyst process.[199]

straight CNTs (Figure 6 B (c)). The stress distributed between the CNTs in the forest during growth kept the straight and curved CNTs growing at the same macroscopic rate. Thus, a synchronous growth of CNT array with pristine stress occurred in the heterogeneous catalyst process.[199] The curvature of curved CNTs can be increased by an external force.[201] High density metal particles and flat substrate are needed for the CNTs to be self-organized into a vertically aligned structure. For instance, when there were round concaves on flat substrates (diameter at around 10 μm), CNTs will self-organize into CNT ropes for further growth. If there were irregular gaps at the sub-micron scale, the initial CNTs get entangled and formed high density agglomerates.[202] Compared with agglomerated CNTs, the CNTs in the array form has an ordered structure, which will release the growth stress due to structure deformation and self organization. Meanwhile, the density of CNTs is decreased, leading to a larger aspect ratio for CNTs.

Based on the CNT growth and agglomeration mechanism, various effective strategies for VACNT mass production have been proposed. One of the first ideas was the synthesis of aligned CNTs on a flat surface. However, the surface area of a flat substrate is often limited, and flat substrates have poor mobility. Only 1 $g\,h^{-1}$ VACNT arrays can be obtained with flat silica as substrate.[101] The quantity of the VACNT arrays is proportional to the surface area of the substrate. If a substrate with a larger surface area is used (e.g., spheres) more VACNT arrays can be produced. In particular, when spheres with diameters of 0.8 mm and a total volume of 1 L were used as the growth substrate, the surface area increased to as much as 7.5 m^2 (equivalent to the surface area of 14500 pieces of one-inch wafer). These spheres exhibited good transportability and could be easily manipulated into and out of reactors. We have recently synthesized VACNT arrays from cyclohexane,[203] liquefied petroleum gas,[204] and ethylene[205] on ceramic spheres.

After 2 h growth, all the spheres exhibited a flower-like structure, with 15–25 mats of long VACNT arrays oriented perpendicular to the surface of the spheres. Other kinds of curved surfaces, such as quartz/SiC/carbon fibers,[206] flakes,[207,208] and microspheres,[209] were also effective for VACNT growth.

To avoid damage caused by the collisions among CNT arrays during transport or fluidization processes, a strategy of intercalating VACNTs into layered compounds and directly constructing a layered hybrid nanocomposite composed of alternate CNT films and inorganic sheets has been proposed (Figure 7).[210] Compared to a flat substrate with low surface area, the lamellar catalysts offer much larger specific surface areas ($>3\ m^2 g^{-1}$) to provide enough surface area for the growth of VACNT arrays. Meanwhile, by crushing and screening, lamellar catalysts that are "A" particles in the Geldart particle classification[211] were produced as the catalyst to simplify fluidized-bed operations. The aligned CNTs can intercalatedly grow within a single lamellar particle, and collisions between CNT arrays during growth are therefore avoided. This was successful for the mass production of VACNT arrays in a fluidized-bed reactor. VACNT arrays with CNT diameters of 7–13 nm and CNT lengths of 0.10–100 μm were intercalated among inorganic layers.[210] A large amount of CNT arrays can be produced in a fluidized bed with a layered catalyst.[113,212] A $3.0\ kg\ h^{-1}$ VACNT array production was achieved in a fluidized-bed reactor with a diameter of 500 mm.[113] The CNTs in the arrays showed good alignment, and could be easily purified.

For the formation of HACNTs, the interactions among CNTs, substrates, and surrounding environment play key roles. The gas flow, which makes the CNTs grow in a way similar to a flying kite, is efficient for superlong CNT growth. The CNT growth rate is very high, and the weight space velocity can reach $10^8 g_{CNT} g_{cat}^{-1} h^{-1}$, which is millions of times that of agglomerated CNTs on a porous catalyst. This can be attributed to the growth mode of the HACNTs, in which the catalyst particles are at the tips of the growing CNTs, and the growth is free of space resistance. However, the density of HACNTs grown directed by gas flow is very low. For the lattice-directed, ledge-directed, and grapho-epitaxy growth of HACNTs, the substrate provides a strong interaction to drive CNTs to grow with a high density, but the lengths of CNTs are mostly short. HACNTs are mainly used in microelectronics. It is anticipated that the most efficient way for the mass production of HACNTs is piecewise on an assembly line, which is compatible with present fabrication technologies in microelectronics. As CNTs in the horizontally aligned array have few defects, they have potential applications as advanced structural and functional materials. Therefore, the synthesis of HACNTs on movable or free substrates to obtain long CNTs is an important development.

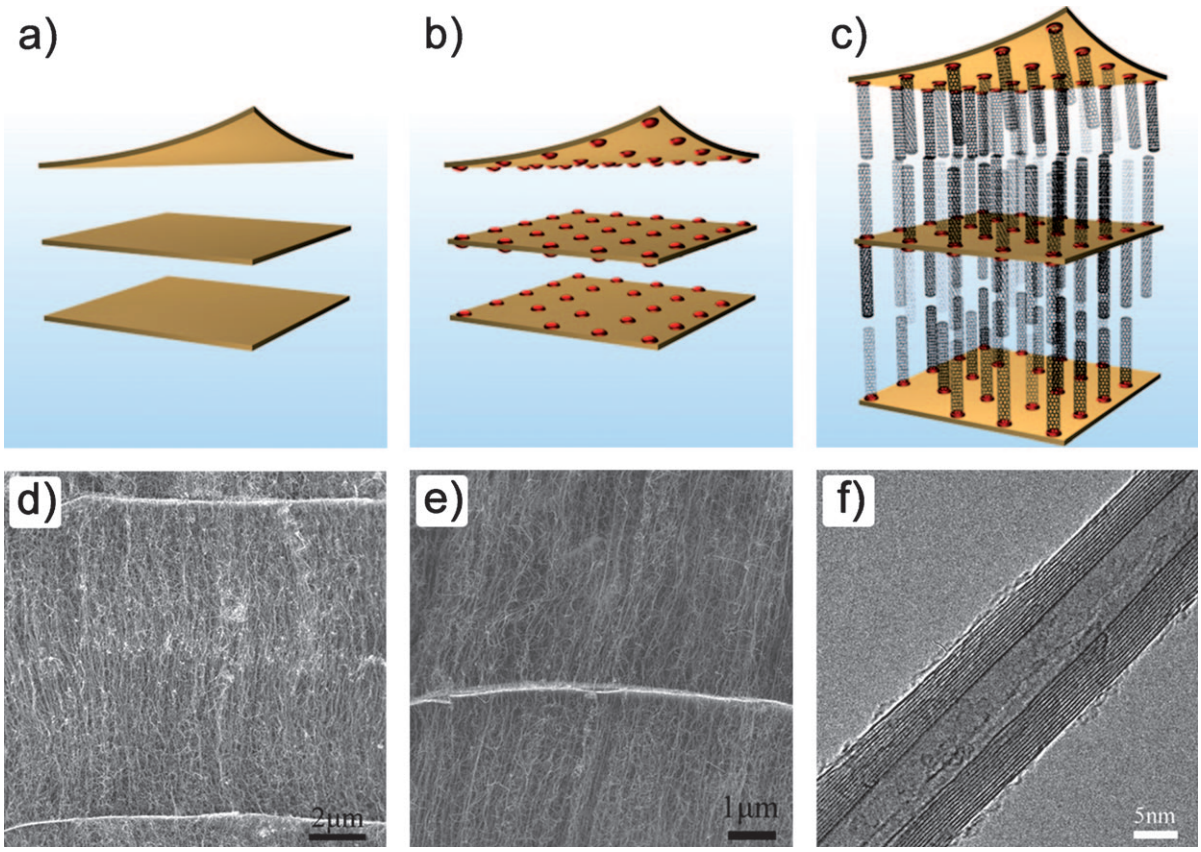

Figure 7. Illustration of the formation of hybrid composites by intercalating vertically aligned CNT films into layered inorganic compounds, showing stacked layers in the original vermiculite (left panel), catalyst particles adhering to the surface of the layers after impregnation (middle), and aligned CNTs between the layers after the CNT growth process (right); d) SEM image showing an enlarged view of a single interlayer with aligned CNTs and an interlayer distance of 20 mm. e) SEM image showing CNT growth on both sides of a vermiculite layer. f) Transmission electron microscopy image of a multiwalled CNT.[210]

3.3. Reactor design: Transport and kinetics

The reactor is the core of an engineering process. Selecting a proper reactor is key to the industrialization of a novel process.[213] Fixed-, moving-, transported-, and fluidized-bed reactors have been developed for CNT production (Table 5). Because CNTs do not exist as a homogeneous medium, unlike traditional products in the chemical industry, selecting a proper reactor type is even more important. For the mass production of CNTs, not only the catalyst, reaction conditions, growth space, and agglomerate control are important, but also other key factors such as uniform temperature and concentration distributions, easy removal of CNTs from the reactor, and maintaining a constant catalyst concentration in the reactor should all be taken into consideration. The ability to quantify kinetic and transport interactions on a variety of scales and using them to assess the effect of reactor performance on the process is very important for designing a proper reactor.[214] In this section, we first address how to select the reactor type. Then the state-of-the-art of transport phenomena and kinetics of CNT growth are summarized. A typical continuous process for CNT production that has been demonstrated on the kilogram scale per hour is discussed.

Table 5. Comparison of different reactor types for CNT production.

	Fluidized bed	Fixed bed	Moving bed	Transported bed I	Transported bed II
Influence on CNT growth	−	−−	−−−	+++++	+++++
Heat transfer	+++++	−−−	−−−	−	+++
Mass transfer	+++++	−−	−−−−	+++	+++++
Flow pattern	well-mixed	piston flow	piston flow	piston flow	piston flow
Temperature control	+++++	−−−−	−−−−	++	++
Scale-up	++++	−−−−	−−−−	−−	+
Usable for agglomerated CNTs	++++	++	+	−	++
Usable for aligned CNTs	+	+	−−	+++	+++++
Achievable capacity	+++++	−−−	−−	++	+++
Continuous production	+++++	−−−−	−−	++	++++

3.3.1. Rector type selection

For agglomerated CNT growth, the development stage of the CNT agglomerates is closely tied to the CNT microstructure because of the different stress states in the CNT agglomerates. The growth space is needed for the increasing volume of the growing CNTs.[215] In a fixed bed, the agglomerated CNTs are packed stationary, which means limited growth space. In this kind of reactor newly grown CNTs have to enter the loose structure of other CNT agglomerates, which causes the intertwining of agglomerates. The reactor then gets jammed, which results in significant flow, heat, and mass transfer problems. The jamming can be solved by keeping the agglomerated CNTs moving in the reactor, because the movement will break the weak connections between the agglomerates so that the growing CNTs in different agglomerates do not get entangled. For example, in a moving bed or transported bed **I** (such as that used in the floating catalyst method for CNT synthesis), the flow pattern of the gas feed is that of piston flow, and CNTs grow only in certain regions of the reactor. When wafers are used as the substrate in a pipeline, the reactor can be considered a transported bed **II**. This is efficient for piece-by-piece synthesis of CNTs on the wafers. In a fluidized bed reactor, the CNT agglomerates are fluidized, and the flow pattern is similar to that of a continuous stirred tank reactor. The fluidized bed reactor offers the good advantages of excellent diffusion and heat transfer rates, ample growth space, ease in scaling up and continuous operation for CNT production. As summarized in Table 5, the most efficient reactor for the mass production of CNTs is the fluidized bed, which has already been adopted worldwide for the commercial production of agglomerated CNTs.

The reactor type also significantly affects the growth of CNT arrays. The properties of CNT array products in a fixed bed reactor showed a distribution along the axial direction.[216] When CNT arrays were grown in a fluidized bed, they had a homogeneous structure, low density, uniform diameter, and few defects, which can be attributed to the available space, uniform temperature and reactant distribution in the fluidized bed reactor.[216] These characteristics of the fluidized bed provided the conditions for the mass production of CNT arrays with uniform properties. For aligned CNTs that are to be grown on wafers piece by piece, the transport bed is the best choice.[15]

3.3.2. Multiphase flow behavior of CNTs

The fluidization of nanoparticles is necessary for continuous handling, good gas–solid contact and mixing, and high mass and heat transfer efficiency, and it is because of these that the fluidized bed is the reactor of choice for providing the conditions for CNT productivity on the ton scale. Preserving the catalyst and CNT product under stable fluidization is a basic issue. To realize this goal, in one aspect, choosing a fluidizable catalyst with a size of 10–200 μm (which could be considered as "A" particles according to Geldart particles classification[211]) is the first step for mass production of CNTs by the fluidized-bed process. This is attributed from the powders in group A exhibit dense phase expansion after minimum fluidization velocity, and this state can be maintained over a large velocity range. In another aspect, the multiphase flow behavior of CNTs has to be well understood for reactor and process design. The expansion behavior of CNT products in a fluidized bed and typical images in the various fluidization regimes are shown in Figure 8.[217] As the gas velocity (U_g) increased, gas channeling occurred first in the bed, and the upper interface of the bed fluctuates strongly (Figure 8a). With $U_g > 0.06\ m\,s^{-1}$, the CNTs began to fluidize (Figure 8b). With $U_g > 0.1\ m\,s^{-1}$, the expansion of the bed slowed and the pressure drop over the catalyst bed remained stable, indicating that fully suspended agglomerates had been formed. Bubble break-up dominated the fluid-

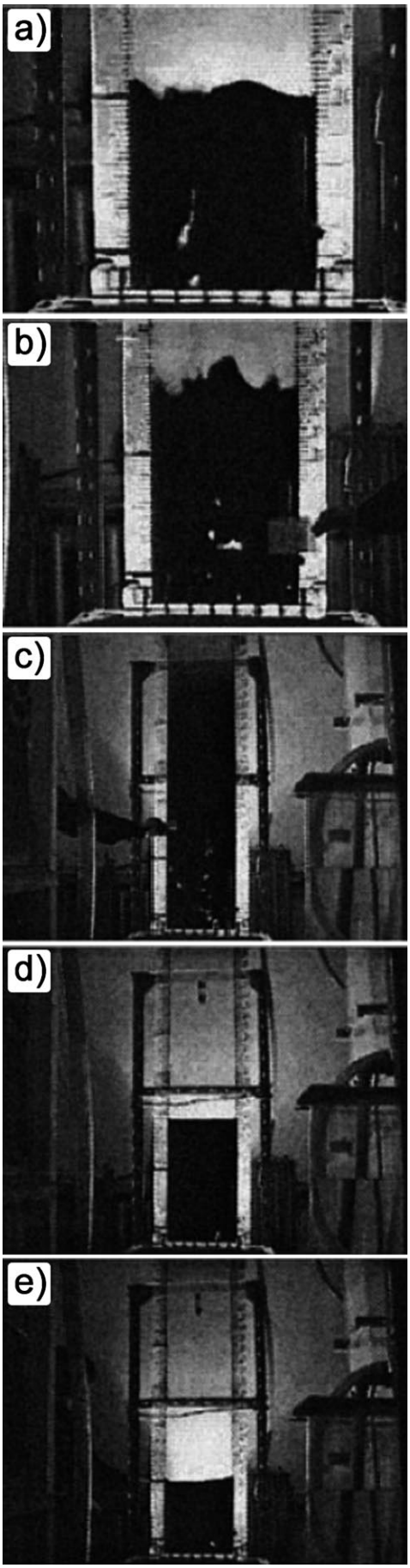

ization, no obvious bubbles could be observed, and the interface with the bed was blurred due to the ejection of particles into the free space (Figure 8c). With $U_g > 0.2\ m\,s^{-1}$, serious entrainment occurred as the bed was operated in fast fluidization. Different height/pressure drop velocity dependences were recorded with decreasing gas velocity from $0.2\ m\,s^{-1}$ to defluidization. A stable agglomerate–bubbling–fluidization could be maintained to $0.038\ m\,s^{-1}$ in the defluidization branch, with slightly changed pressure drops. Below $0.038\ m\,s^{-1}$, smooth particulate fluidization was observed (Figure 8d). This particulate fluidization could be maintained in the range of 0.017–$0.038\ m\,s^{-1}$, and the bed height decreased with the deceasing gas velocity. When the gas velocity was lower than $0.017\ m\,s^{-1}$, channeling appeared again and the bed defluidized (Figure 8e). A smooth and highly expanded fluidization was achieved, but a strong hysteresis existed in the CNT fluidization curve. The fluidization hysteresis can be explained by that different energy was required for the initial fluidization of the beds and suspending of the fluidizing agglomerates, which was connected with the complex surface structure and entangled chain-like network of the CNTs.

The particulate fluidization was not always uniform, and it depended on the gas velocity. In aggregative fluidization, the distribution of the time-averaged solid fractions also showed a stronger radial non-uniformity than Geldart-A particles. Analysis of the transient density signals indicated non-uniformity in the radial solid distribution with strong aggregation among the agglomerates near the wall. However, on the microstructure scale, the gas–CNT flow was more homogeneous than Geldart-A particle fluidization. This was due to the small density difference between the bubble phase and emulsion phase, which was about one order of magnitude smaller than that of fluid catalytic cracking fluidization. Then, turbulent heat and mass transfer were reduced. This points to the fluidized bed reactor as a good choice for the mass production of CNTs.

3.3.3. Kinetics of CNT growth

Chemical kinetics include investigations of how different experimental conditions influence the speed of a chemical reaction and yield information about the reaction mechanism and transition states. It is always desirable to design a reactor and optimize the operation in a cost-saving way. Various apparent kinetic models have been proposed based on the experimental data. For instance, Ni et al. found that the rate of CNT synthesis was proportional to the CH_4 pressure.[218] Pirard et al. conducted a kinetic study on the formation of MWCNTs and found the best models assumed that the elimination of the first hydrogen atom from adsorbed ethylene was the rate-determining step. The activation energy and ethylene adsorption enthalpy were found to be 130 and $-130\ kJ\,mol^{-1}$, respectively.[219] Philippe et al. have produced CNTs with high selectivity by fluidized-bed catalytic CVD. The apparent partial orders of reaction

Figure 8. Fluidization in the various regimes recorded with a 2D bed showing a) channeling, b) agglomeration–bubbling–fluidization, c) turbulence, d) particulates, and e) defluidization.[217]

for ethylene, hydrogen, and iron were found to be 0.75, 0, and 0.28, respectively.[220] Simulation showed that the productivity of MWCNTs can reach 8 kg h^{-1} in a 45 cm diameter reactor operated under semi-batch conditions.[221]

In the growth of aligned CNTs, the CNTs have similar lengths, and it is easy to design in situ methods to monitor the kinetics of aligned CNT growth.[222,223] The growth mark method was used to record the growth rate of aligned CNTs by adding marks during the growth process.[224] It was found that the growth rate was higher in the initial stage and then reached a constant value when the growth temperature was 953 K. Along with increasing C_2H_2 partial pressure, the axial growth rates also increased, which indicated that the reaction cannot be zero-order in C_2H_2.[224] In fact, the decomposing mechanism of a hydrocarbon at high temperature is complex, and the elementary reactions should be determined first. If the catalyst has a constant activity, then a linear growth behavior of aligned CNTs is obtained.[225,226] The relationship between the length of CNTs and the growth time can be expressed as:

$$L = rt \quad (1)$$

where L is the length of aligned CNTs, t is the growth time, and r is the growth rate of VACNTs, which varies from 0.05–20 μm min^{-1}. For HACNTs, the rate of CNT growth can reach 4800–5600 μm min^{-1}.

If the initial growth rate is proportional to the carbon source concentration and the rate-determining step is the carbon source decomposition,[197,225,227,228] the length of aligned CNTs can be expressed as:

$$L = \sqrt{\left(\frac{D_e}{k_s}\right)^2 + \frac{2D_eC_0}{a}t} - \frac{D_e}{k_s} \quad (2)$$

where D_e is the effective diffusion coefficient, k_s is the surface rate constant for reacting the carbon source to CNT, C_0 is the feedstock concentration, and a is a structure-dependent constant of the CNT array.[228]

If the catalyst is continually poisoned due to the formation of a carbonaceous layer around the catalyst nanoparticles, or reactions involving byproducts, the rates of these catalyst decay processes will be proportional to the rate of the synthesis reaction. The growth behavior of aligned CNTs can be expressed as:

$$L = \beta\tau(1-e^{-t/\tau}) \quad (3)$$

where β is the initial growth rate and τ is the characteristic catalyst lifetime.[223,229]

Linear growth of aligned CNTs was widely observed during the first growth stage. When the CNTs become longer, either the carbon source diffusion or catalyst decay was described, and this is highly dependent on the catalyst preparation and growth parameters. The possible rate-determining steps of CNT growth are hydrocarbon decomposition,[197,225,227] catalyst activity,[223,229] and diffusion of carbon into the catalyst particles.[198,224,230] Both the kinetic and the rate-determining step of CNT growth varies with different catalysts and growth parameters.[225,228,231] It is important to test the kinetics by experimental results and select the appropriate kinetic model for further scaling up. For thermal CVD growth, not only catalytic hydrocarbon decomposition, but also thermal decomposition of hydrocarbon was observed, which induced the deposition of graphene segments on the outer walls of the CNTs. This led to the increasing of the outer diameter of the CNTs grown.[232]

With continual growth of CNTs, the metal nanoparticle catalyst will lose its activity gradually because of sintering, encapsulation, poisoning, limited space for CNT extension, and other reasons. Usually, billions of CNTs are simultaneously grown in each batch, and the reason for the "death" of each catalyst particle can be different. This strongly depends on the growth evolution and environment. In a recent work on the growth behavior of aligned CNTs, it was found that aligned CNT growth terminated abruptly after exhibiting a steady decay in growth rate.[233] Structural disorder is a distinct chemical and/or mechanical signature of self-terminated CNT array growth.[233] Bedewy et al. reported a four-stage growth of aligned CNTs: (i) self-organization; (ii) steady growth with a constant CNT area number density; (iii) decay with a decreasing area number density; and (iv) abrupt self-termination, which is coincident with a loss of alignment at the base of the forest.[234] The abrupt termination of CNT array growth was considered to be caused by the loss of the self-supporting structure, which is essential for the formation of a CNT array. This event was triggered by the accumulating growth termination of individual CNTs.[234] Kim et al. reported that the termination of aligned CNT growth can be intrinsically linked to the evolution of the catalyst morphology. A combination of both Ostwald ripening and subsequent subsurface diffusion led to the loss of the iron nanoparticle catalyst, and this correlated with the termination of CNT growth.[235] Very recently, after applying a transformation based on high-resolution spatial mapping of alignment, the length kinetics curve was found to be linear until self-termination, even after the slope of the height kinetics began to decrease.[236] By considering feedstock and byproduct diffusion in the root growth of aligned CNTs, it was shown that MWCNT arrays were usually free of feedstock diffusion resistance while SWCNT arrays suffered from strong diffusion resistance.[228] Thus, delivery of gases by a gas shower system from the top of the array, enabling direct and precise supply of carbon source and growth enhancer to the catalysts, is an efficient way for large-area growth of vertically aligned SWCNTs.[15] A stable laminar flow on the substrate was always the basis for ultralong horizontally aligned CNT growth via gas-flow-assisted CVD.[151]

3.3.4. Process design for the continuous production of CNTs

Based on the catalytic process, transport phenomena, and understanding of the kinetics of CNT growth, process design, including capital and operating cost, operation mode (semi-batch, batch, or continuous), and production and purification methods, can be performed. An understanding of process design is the first step for scaling up and commercialization.

Agboola et al. presented this for a high-pressure carbon monoxide plugflow process and CoMo catalyst fluidized-bed process recently.[237] In this section, the nano-agglomerated fluidized bed process for FloTube production was selected as a representative process to illustrate the continuous operation of CNT production.

The catalyst is first reduced and then transferred into the main fluidized-bed reactor. A gas mixture containing the carbon source reactant is introduced into the bottom vessel of the reactor, and passes through the gas distributor, the fluidized bed, and finally flows out into the atmosphere. With continuous growth of CNTs, the catalyst deactivates gradually, and the conversion of the carbon source decreases accordingly. To achieve the continuous production of CNTs, fresh catalyst has to be added. It should be noted that the density of the catalyst is 5–15 times higher than that of the CNT products, thus their fluidization behaviors vary significantly. If the fluidized bed were operated in the regime for CNT catalyst fluidization with a high gas velocity, most CNT products will be blown out from the reactor, which should be avoided. Similarly, if it were operated in the regime for CNT product fluidization with a low gas velocity, most CNT catalyst particles will be defluidized and fresh catalyst cannot be effectively used. To provide a robust process for continuous production, a multistage reactor consisting of two or more fluidized bed reactors, or multizone fluidized bed reactors, was proposed.[238] The fresh catalyst and final products were operated in different reactors or zones to keep all of them in good fluidization states. Both the catalyst and products can be in situ transferred between different reactors, and CNTs were continuously produced in this process. A pilot plant fluidized-bed reactor with a diameter of 500 mm was used for the mass production of agglomerated CNTs and VACNTs (Figure 9b).

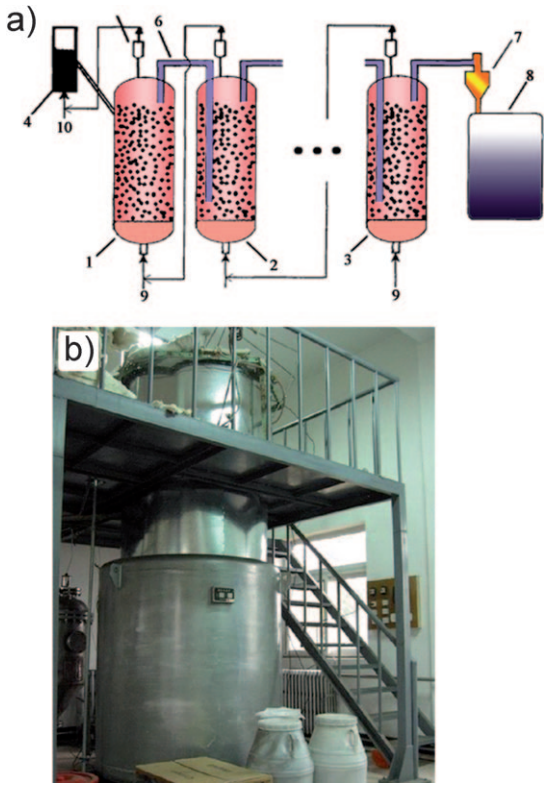

Figure 9. a) Continuous mass production of CNTs. 1: first reactor; 2: second rector; 3; last reactor; 4: catalyst reduction reactor; 5: gas–solid separator; 6: overflow pipe; 7: cyclone; 8: CNT tanker; 9: connection between reactors; 10: catalyst inlet. b) Pilot plant facility for CNT production (Reproduced with permission from Ref. [21]. Copyright 2008 Elsevier.).

3.4. Process Intensification for the CNT industry

In modern chemical engineering and process technology, process intensification involves the development of innovative machines and techniques that give improvements in manufacturing and processing, substantially decreased equipment volume, energy consumption, or waste formation, and ultimately leads to cheaper, safer, and sustainable technologies.[239] Process intensification is based on maximizing the effectiveness of intra- and intermolecular events to give each molecule the same processing experience, optimizing the driving forces at every scale and maximizing the specific surface area to which these forces apply, and maximizing the synergistic effects from component processes.[240] To produce CNTs and utilize them in a cheaper, safer, and more sustainable manner, researchers, especially those with a chemical engineering background, have developed novel process intensification technologies. To cross the scales of CNT production and eliminate the bottlenecks in the CNT industry, various strategies were proposed as bridges between atomic self-assembly, agglomerate formation and evolution, hydrodynamics of nanomaterial flow, delivery, and their applications, among which strong couplings always exist. The formation of CNTs with a desired nanostructure depends not only on the catalyst at the atomic scale, but also on the agglomeration behavior at the mesoscale, and multiphase flow, heat and mass transfer of catalysts and products at the reactor scale. The decoupling of the interactions between the different scales is the first step. Due to its strong interdisciplinary character, especially for novel nanomaterials, process intensification is used to meet these challenges in collaboration with other disciplines, such as chemistry, catalysis, applied physics, materials engineering, electronics, etc. In this section, the discussion of the state-of-the-art of CNT process intensification is classified by molecular scale intensification, feedstock saving, multifunctional reactor, and coupled process development aspects.

3.4.1. Catalysis route innovation

Additives can significantly improve the activity of catalysts for efficient growth of CNTs. To improve the yield of CNTs and synthesize SWCNTs and DWCNTs, sulfur or sulfur-containing compounds (such as thiophene and H_2S) have frequently been used as additives in the floating catalyst CVD method. It was found that the addition of sulfur results in localized liquid zones on the surface of large catalyst particles as the initial nucleation sites and the shell number of CNTs can be changed at the nucleation and growth stages.[241] Thus, high-quality CNTs

with tunable diameters can be obtained.[242] Long nanotube strands consisting of aligned SWCNTs with lengths up to several centimeters can also be synthesized.[67,193,243] Moreover, oxidative gases, such as H_2O,[14,160,244,245] CO_2,[191,246,247] or O_2,[248] were shown to give extraordinary enhancement for high-purity CNT growth. Water (175 ppm) was an efficient additive for the supergrowth of aligned SWCNTs.[14] When an oxidative gas was added into the reactor, not only amorphous carbon was suppressed, but also the activity of catalyst was greatly improved.[245] Futaba et al. reported that the key to a highly efficient growth of CNTs includes two essential ingredients in the growth ambience: a carbon source that does not contain oxygen and a minute quantity of a secondary gas, which does contain oxygen that acts as a growth enhancer.[249] In this situation, high density nanoparticles with good stability can be formed, which is the basis for the continuous growth of super long CNTs. This is a very easy way to enhance S-/DWCNT production. For example, Wen et al. found that a small amount of CO_2 was effective for removing amorphous carbon to regenerate the catalyst, decrease the size of the MgO support and increase the specific surface area of the Fe/Mo/MgO catalyst.[191] Huang et al. observed the morphology evolution with different added CO_2 amounts and reported these were from convex- to radial-block- and then to bowl-shaped during thermal CVD. Meanwhile, with the introduction of CO_2, carbonaceous impurities were eliminated and the wall number of CNTs was also significantly reduced.[247]

Moreover, the CNT structure can be changed by the introduction of a catalyst precursor as simple molecular scale process intensification. For example, the dense fluidized bed and floating catalyst CVD methods can be combined to decompose propylene with CNTs as support and metal particles from the in situ pyrolysis of ferrocene as the catalyst. Short and thin CNT branches can be constructed on the tips or sidewalls of the CNTs.[250] Wei et al. reported a magnetism-assisted CVD method in which the external magnetic field promoted the coalescence or division of the magnetic catalyst particles, causing the formation of branched or encapsulated CNTs.[251] Multibranched CNT arrays can be obtained using flow fluctuation by a branching mechanism of fluctuation-promoted coalescence of catalyst particles.[252] The branched CNTs obtained can be used as intermolecular junctions components, which not only connected different CNTs for integration, but also can act as functional building blocks in circuits, for example rectifiers, field-effect transistors, switches, amplifiers, and photoelectrical devices.[253] If the carbon source was replaced by an nitrogen-containing carbon source, CNTs with the bamboo structure,[254] or nitrogen-doped CNTs can be obtained.[255] Nitrogen-doped CNTs show tunable properties; in particular, chemically inert CNTs were chemically active after the doping of nitrogen atoms.[255] Other element-doped CNTs, such as those doped with phosporus[256] or boron,[257] also show unique properties and wide applications in catalysis, energy conversion, and energy storage, and can also be easily obtained by process intensification during CNT synthesis.

3.4.2. Feedstock saving

For a chemical process, 60–90% of the production cost comes from the raw materials. Selecting proper feedstocks is also a key factor for the efficient production of CNTs at low cost. For the CVD process, the yield of carbon is the key factor for the economical production of CNTs. Investigations into new inexpensive feedstocks and more efficient catalyst/support combinations suitable for the mass production of agglomerated and aligned CNTs are needed. The growth of CNTs on natural materials is a potential way to achieve environmentally benign and low-cost production.[258] A variety of minerals (such as volcanic lava rock, bentonite, soil,[258] garnet sand,[259] wollastonites,[260] montmorillonite,[261] sepiolite,[262] and vermiculite,[113,210,212]), biomass-derived materials (such as activated carbon,[263] black jew's-ear fungus and black sesame seeds[264]), and industrial wastes (such as red mud[265] and fly ash[266]), have been used as catalysts and/or catalyst supports for the synthesis of CNTs. Organic natural materials, such as coal,[267] natural gas,[268] liquefied petroleum gas,[269] eucalyptus oil,[270] turpentine oil,[271] camphor,[272] deoiled asphalt,[273] even grass,[274] can serve as the carbon source for CNT synthesis. Some natural carbon sources contain impurities (such as S, As, P) that can poison the metal catalyst, but other impurities are efficient for CNT growth as enhancers. It is still difficult to get CNTs with high purities and ideal structures in high yields, and exploring effective natural feedstocks is a possible solution. Using renewable energy for CNT synthesis is also a goal. For example, concentrated solar radiation has been used as a clean source of process heat for the production of CNTs.[275] With recent rapid progress in energy conversion and storage, it may be more economical to turn solar energy into electricity for the synthesis of CNTs, which will further promote the production of CNTs in a sustainable way.

3.4.3. Multifunctional reactors

The industrial reactor type and its operation regimes are mainly determined by the CNT growth mode and agglomeration behavior. Compared with the fixed-bed, moving-bed, and transported-bed reactors, the fluidized-bed reactor has excellent heat and mass transfer properties and good mixing behavior, which is of paramount importance for the mass production of CNTs. CNT production in a fluidized-bed reactor has to go through a series of steps, including catalyst reduction, CNT growth, catalyst support crushing, CNT agglomerate formation, and so on. For an effective process, the changes in for example reactant concentration, density of solids, catalyst deactivation, and particle size growth, which significantly influence the operation, have to be considered. By doing so, an enhancement can be achieved in the reactor operation by the use of a coupled CVD process in a coupled fluidized bed. For example, a two-stage fluidized bed has been used to produce CNTs that gave a higher conversion of the reactant. For methane decomposition in a two-stage fluidized bed reactor, a lower stage at low temperature and an upper stage at high temperature are commonly used. This allows the methane to decompose on

fluidized catalyst particles with high activity at a high temperature condition. The carbon produced diffuses into the catalyst particles, which flow between the stages, to form CNTs in both the low- and high-temperature regions. Therefore, the catalytic cycle of CNT production and carbon diffusion on the microscopic scale can be tailored by a macroscopic method when multi-functional reactors are adopted for CNT production. The multistage operation with different temperatures in different parts of a fluidized-bed reactor is an effective way to meet both the requirements of hydrogen production and preparation of CNTs with relatively good crystallinity.[276] Thus, there is enough scope for process intensification on the reactor scale.

3.4.4. Coupled process development

Chemical engineering scaleup aims to develop a high efficiency process and is an example of complex system engineering. Here, the coupling of the catalyst and reactor operations is an important aspect to achieve process intensification of CNT production.

The coupled process can be designed at the atomic scale. For example, the decomposition of CH_4 is an endothermic reaction with a reaction heat of 75 kJ mol^{-1}. The decomposition of C_2H_4 and C_2H_2 are exothermic reactions with reaction heats of 52 and 269 kJ mol^{-1}, respectively. Thus, the presence of C_2H_4 or C_2H_2 would increase the conversion of CH_4 by 3 to 5 times, which has been used to significantly increase the production rate of CNTs from 20–30 to 45–75 g g_{cat}^{-1} h^{-1} at 723–873 K.[277] This enabled the catalysis of CH_4 activation at low temperature to produce H_2 and CNTs with high efficiency. The H_2 produced was free of CO, which was a good H_2 source for a proton exchange membrane fuel cell.[278] Secondly, a coupled process can also be designed in which both catalyst reduction and CNT growth were considered. It was noted that the catalyst was originally in the oxide state and reduction was necessary before CNT growth. And the decomposing of a carbon source, such as methane, into CNTs and hydrogen will need external heat. This can be supplied in part by catalyst reduction that release heat, and which would further contribute to the breaking of the methane decomposing equilibrium by the consumption of hydrogen.[279] The combination of catalyst reduction and methane decomposition is a good way to increase the yield of CNTs. Thirdly, the growth of high purity CNTs and the facile release of them from the substrate can be simultaneously achieved by a CO_2 oxidation process. CO_2 is often selected as the oxidant mainly due to the convenience of its use in industrial applications and its proper oxidizing ability for the partial oxidation of CNTs. The introduction of CO_2 after the growth of CNT arrays can significantly weaken the array-substrate interaction and selectively etch away amorphous carbon decorated on the CNTs. This simple oxidation approach was found to be suitable to release aligned CNTs from various substrates to give free standing CNT arrays. As shown in Figure 10, free standing CNT arrays can be easily released from spherical ceramic substrates with CO_2 oxidation.[280] During the radial growth on ceramic spheres, CNT arrays split into CNT pillars on the spherical substrate. After the oxidation, the connection between CNT pillars and the substrate was weakened and a mechanical force could be applied to bring about the separation.[280]

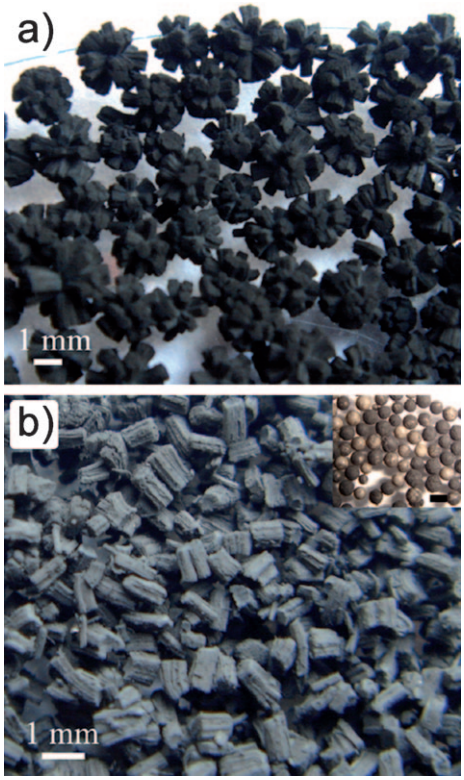

Figure 10. a) CNT arrays grown on ceramic spheres, showing radial growth behavior. b) Release of CNT arrays by simple mechanical vibration after CO_2 oxidation. The inset shows the bare ceramic spheres after the detachment of CNT arrays.[280] The scale bar in the inset is 1 mm.

3.4.5. One-step synthesis route for direct CNT application

The applications of CNTs that use large volumes of CNTs commonly require tedious procedures in the CNT manufacturing process that include separation, purification, dispersion, and combination to form a composite with other materials, such as polymers, metals, ceramics, and electrode materials. This is because that in most cases, CNTs have to be supplied in high purity form, which are then mixed into a matrix to make multifunctional composites. Thus, the direct synthesis of CNT structures for some applications to avoid these procedures is of great interest. If the CNTs can be in situ grown in the positions required in or among the materials of the composites, such as metal (Al),[281] ceramic,[282] clay,[113,210,212,261] fiber (SiC, carbon fiber),[206,283] advanced composites can be produced directly for specific composite applications. If CNTs can be directly grown on conductive substrates (e.g., glass carbon,[284] Ta,[284] Cu,[285] Al film,[286] inconel alloy,[287] graphite spheres[288]), the CNTs obtained can be used directly as electrodes for energy conversion and storage applications.[289] The CNT composites obtained can even serve as field emission display devices,[24] filters,[290] and cushion materials.[210,291] Various potential applications that use directly synthesized CNT architectures for heat dissipation,[292]

nano Faraday coil,[208] fillers for advanced mechanical and heat transfer composites,[293] have also been proposed. CNT nanowoven cloths,[294] CNT strands,[67,193] CNT buckybooks,[295] and CNT yarns/sheets[296] obtained from aligned CNTs are also good examples to demonstrate the mechanical property of CNTs for advanced applications in aerospace and energy conversion. It should be noted that one-step synthesis route gives CNTs with specific organization and alignment, which avoids tedious post treatment procedures in a liquid phase, and is a good candidate for CNT commercialization.

3.5. CNT mass production and commercialization

A discussion of the engineering science based on a multiscale space–time analysis was introduced in the second section to give a guideline for the scale up of a CNT synthesis route. It is hoped this would provide a strong technological impetus for CNT commercialization. On the other hand, the commercial success of a material requires a level of consistency and quality that can only be assured by internationally agreed upon standards of measurement. CNT standardization, including terminology, standard measurement practices, and quality evaluation of the supplies are desired. Since 2007, workshops of the International Workshop on Metrology, Standardization and Industrial Quality of Nanotubes have been organized at the annual International Conference on the Science and Application of Nanotubes. In China, standards for MWCNTs and test methods for purity of MWCNTs were announced on October 30, 2009 and validated for use from June 1, 2010 with Standard GB/T 24491-2009 and GB/T 24490-2009, respectively. Terminology, classification, test methods, inspection rules, packaging, marking/quality certification, storage, transportation, and safety precautions for MWCNTs are given in the GB/T 24491-2009 Standard. A combination method based on carbon burning, thermal gravimetric analysis, transmission electron microscopy characterization, and photo image analysis techniques is to be used to measure MWCNT purity in the GB/T 24490-2009 Standard. From the proposal by ISO/TC 229 and IEC/TC 113 Joint Working Group 1, a technical specification on the vocabulary for carbon nano-objects was published as ISO TS 80004-3 on April 19, 2010. These efforts at standardization will help with individual commoditization, compatibility, interoperability, safety, and reproducibility of CNTs. More standards on SWCNTs, aligned CNTs, and detailed characterization of CNTs are still urgently required.

Various CNT (especially for agglomerated CNTs) industrial processes and their commercialization have been successfully realized worldwide. For CNT CVD production, the producers are mainly in China, Japan, United States, Germany, France, Belgium, and Korea.[17] The arc discharge synthesis of SWCNTs is also an important way to produce high quality CNTs, which was well illustrated by Ando's group in Japan,[297] and Chen's group[298] in China. The wafer scale growth of VACNTs developed by Fan's group[24] at Tsinghua University in China and Hata's group[14] at Advanced Industrial Science and Technology have been scaled up. A recent work showed that aligned CNTs can be intercalatedly grown in the layered structure of natural clay in a fluidized bed at a scale of 3.0 kg h^{-1}.[113] There are now enough M/SWCNTs available in the markets, which should be a big help in the exploration of CNT applications. With the rapid development of mass production technology, the price of CNTs has decreased rapidly. Ten years ago, the price of CNTs was higher than that of gold (45 \$ g^{-1}). Today, the prices of MWCNTs and SWCNTs are in a range of 0.2–25 and 50–400 \$ g^{-1}, respectively, which are still higher than that of carbon nanofibers (0.1–5 \$ g^{-1}). The prices for specialty CNTs, such as enriched semiconducting and metallic SWCNTs (ca. 500 \$ mg^{-1}), length- and surface-functionalized CNTs, and doped CNTs, are still extremely high. A straight line is approximately obtained for a double logarithmic coordinate plot of the productivity and prices of S-/MWCNTs for high-end application. Presently, the high price of CNTs is mainly contributed from the high costs of the CNT process and product purification, high equipment cost, limited scalability of manufacturing methods, and low productivity. The large price range is due to differences in product yield of the different CNT production methods. It can be anticipated that the price of CNTs will further decrease to those that would meet the market price acceptable by the end-user application. However, the CNTs available are still more expensive than bulk chemical products and other raw materials (such as carbon blacks, polyethylene, polypropylene, etc.). In addition, quality and reproducibility are still quite important issues. The design of novel catalytic routes for CNTs with specific structure and their scale up are still big challenges.

4. Summary and Outlook

During the last two decades research on nanocarbon materials, from fullerenes to CNTs and graphene, has been a focus of the nanosciences. As a man-made material, thorough investigations into the properties of CNTs and into their large-scale application are only possible when they are available in large amounts. Large-volume applications (e.g., composites, energy conversion and storage) require large amounts of CNTs of good quality, while limited-volume applications require high structure and reproducibility standards. Achieving the growth of high-quality CNTs at a low cost and on a large scale has been a problem in the past 20 years. The problem has been explored by many groups, which have looked at fundamental science, engineering science, scale-up technology, and commercialization.

The growth of CNTs and their mass production are self-assembling processes that have to be scaled up across diverse space–time scales. A scalable route, from carbon-atom self-assembly at the atomic scale, CNT organization at the mesoscale, to CNT fluid mechanical properties and kinetics at the reactor scale, process design and intensification at the facility scale, and environmental, health, safety, and ecological at the global scale has been developed for the production of agglomerated and aligned CNTs. With process intensification technology, such as catalyst route innovation, feedstock saving, and a coupled process, the quality of CNTs has been improved and the cost of CNT production decreased. The length of CNTs can

reach 20 cm in HACNT arrays, and some routes have been proposed for chirality-selective growth of SWCNTs. However, the control of the structure of individual CNTs is still limited. The control of the chirality, defect density, open/close ends, growth rate, and CNTs with the same length and wall number are still problems. Understanding the growth mechanism of CNTs grown on catalysts and their agglomeration behavior is the key to achieve these goals. Some of the aims of CNT synthesis, such as super long CNTs, super aligned CNTs, reproducible CNTs with the same length and wall number, require an integrated process that not only involves the growth mechanism on a catalyst, but also involves the preparation of identical metal catalysts and preservation of their sizes during CNT growth. With the wide availability of CNTs as a platform, it should be possible to develop more new CNT based compounds by doping, grafting, and hybridization. Effective solutions will have to be generated by the integration of CNT synthesis chemistry, CNT interaction physics, and chemical engineering science.

Agglomerated S-/MWCNTs and aligned MWCNTs have already been widely used in Li-ion batteries, electrical conductive fillers, and advanced nanocomposites. The needs of large volume CNT applications are still increasing, and 1000 tons per year of CNTs produced should happen within two years, and a 10000 tons per year scale CNT production technology could be built within five to ten years to mass produce CNTs in bulk amounts. If bulk quantities of CNTs become available in the markets, the price of CNTs will further decrease to near that of engineering plastic, and nanocomposites with rubber/plastic/ceramic/metal matrices with advanced properties can be commercialized then. Aligned SWCNTs with extremely high quality have been produced, and their scale up is underway. A ton-scale market for aligned SWCNTs would form and advanced composites and energy conversion devices would be possible. With the progress on growing superlong CNTs, their use for making strong fibers could be realized. If the chirality of CNTs can be controlled, microelectronic applications based on the 1D nanocarbon would flourish.

However, it should be noted that as compared with traditional bulk chemicals, CNTs are far from large-scale applications (millions of ton scale) because of the difficulty in both the synthesis and the subsequent product treatments. One main difficulty is the strong coupling between CNT structures, their production process, and their properties. Other difficulties are the tedious procedures in the post treatment process, such as dispersion, forming of composite, and others, which are even more difficult. It is still hard to determine whether a process with separated or integrated synthesis and assembling would be more efficient. This kind of complex coupling requires engineers to develop the production route for the products with an integrated whole view of all the steps throughout the synthesis and applications of CNTs rather than a view on only one scale.

As a novel industry, engineering considerations are still required to be provided for a sustainable development of the CNT industry. The toxicity of pure CNTs has not been well researched. To maintain the sustainable development of the CNT industry, international standards for CNTs and related analysis methods should be set up. The establishing of a government–worker–industry partnership is a big step for worker protection. An intrinsically safe process with high efficiency and good economics is needed.

Agglomerated CNTs and aligned CNTs have been successfully mass produced on the ton scale, and are readily available on the market. As a typical nanomaterial, the CNT is a model that demonstrates the power of nanotechnology. It is also a great platform for scientist to use to explore nanoscience and engineers to develop advance devices. As a cutting edge material, CNTs will play an even more important role in the sustainable society.

Acknowledgements

The work was supported by the Natural Scientific Foundation of China (20736007, 2007AA03Z346) and the China National Program (2011CB932602).

Keywords: carbon nanotube · catalysis · chemical engineering · chemical vapor deposition · mass production

[1] a) L. V. Radushkevich, V. M. Lukyanovich, *Zurn. Fisic. Chim.* **1952**, *26*, 88–95; b) A. Oberlin, M. Endo, T. Koyama, *J. Cryst. Growth* **1976**, *32*, 335–349; c) M. Monthioux, V. L. Kuznetsov, *Carbon* **2006**, *44*, 1621–1623.

[2] S. Iijima, *Nature* **1991**, *354*, 56–58.

[3] a) M. Endo, M. S. Strano, P. M. Ajayan, *Top. Appl. Phys.* **2008**, *111*, 13–61; b) J. M. Schnorr, T. M. Swager, *Chem. Mater.* **2011**, *23*, 646–657.

[4] H. G. Tennett, (Hyperion Catalysis Int.) WO8603455A1, **1986**.

[5] a) M. Endo, *Chem. Tech.* **1988**, *18*, 568–576; b) M. Endo, K. Takeuchi, S. Igarashi, K. Kobori, M. Shiraishi, H. W. Kroto, *J. Phys. Chem. Solids* **1993**, *54*, 1841–1848.

[6] a) D. E. Resasco, B. Kitiyanan, J. H. Harwell, W. Alvarez, D. Jang, W. E. Alvarez, J. E. Herrera, L. Balzano, D. Resasco, J. Harwell, (Univ Oklahoma) WO200073205A, **2007**; b) D. E. Resasco, B. Kitiyanan, W. Alvarez, L. Balzano, B. Kitivanan, W. E. Alvarez, (Univ Oklahoma) WO200194260A, **2001**; c) D. E. Resasco, B. Kitiyanan, W. E. Alvarez, L. Balzano, (Univ Oklahoma) US2006039849A1, **2006**.

[7] W. E. Alvarez, B. Kitiyanan, A. Borgna, D. E. Resasco, *Carbon* **2001**, *39*, 547–558.

[8] R. E. Smalley, K. A. Smith, D. T. Colbert, P. Nikolaev, M. J. Bronikowski, R. K. Bradley, F. Rohmund, R. Smalley, K. Smith, D. Colbert, (Univ Rice) WO200026138A, **2000**.

[9] P. Nikolaev, M. J. Bronikowski, R. K. Bradley, F. Rohmund, D. T. Colbert, K. A. Smith, R. E. Smalley, *Chem. Phys. Lett.* **1999**, *313*, 91–97.

[10] F. Wei, G. Luo, Y. Wang, H. Yu, Z. Li, W. Qian, Z. Wang, Y. Jin, (Tsinghua Univ) WO200294713A, **2002**.

[11] Y. Wang, F. Wei, G. H. Luo, H. Yu, G. S. Gu, *Chem. Phys. Lett.* **2002**, *364*, 568–572.

[12] a) M. Bierdel, S. Buchholz, V. Michele, L. Mleczko, R. Rudolf, M. Voetz, A. Wolf, *Phys. Status Solidi B* **2007**, *244*, 3939–3943; b) S. Buchholz, D. G. Duff, V. Michele, L. Mleczko, C. Muennich, R. Rudolf, A. Wolf, D. Gordon, D. Duff, M. Volker, M. Leslaw, M. Christian, R. Reiner, C. Munnich, (Bayer Material Science AG) WO2006050903A2, **2006**; c) S. Buchholz, V. Michele, L. Mleczko, C. Muennich, R. Rudolf, A. Wolf, Leslaw, C. Munnich, (Bayer Material Science AG) WO2007093337A2, **2007**; d) R. Bellinghausen, S. Buchholz, V. Michele, L. Mleczko, A. Wolf, J. Buhiholcheu, R. Meulrekcheuko, P. Mihel, D. E. Wolf A, D. E. Buchholz S, D. E. Michele V, D. E. Mleczko L, D. E. Bellinghausen R, (Bayer Material Science AG) WO2009043445A1, **2009**.

[13] K. Hata, S. Yasuda, M. Yumura, (NIIT) WO2008096699A1, **2008**.

[14] K. Hata, D. N. Futaba, K. Mizuno, T. Namai, M. Yumura, S. Iijima, *Science* **2004**, *306*, 1362 – 1364.
[15] S. Yasuda, D. N. Futaba, T. Yamada, J. Satou, A. Shibuya, H. Takai, K. Arakawa, M. Yumura, K. Hata, *ACS Nano* **2009**, *3*, 4164 – 4170.
[16] a) K. Jiang, S. Fan, Q. Li, F. Y. Fan, (Tsinghua Univ) US2004053780A1, **2004**; b) X. B. Zhang, K. L. Jiang, C. Teng, P. Liu, L. Zhang, J. Kong, T. H. Zhang, Q. Q. Li, S. S. Fan, *Adv. Mater.* **2006**, *18*, 1505 – 1510.
[17] World Technology Evaluation Center-Inc., WTEC Workshop International R&D of Carbon Nanotube Manufacturing and Applications, **2006**.
[18] a) H. J. Dai, *Top. Appl. Phys.* **2001**, *80*, 29 – 53; b) C. N. R. Rao, B. C. Satishkumar, A. Govindaraj, M. Nath, *ChemPhysChem* **2001**, *2*, 78 – 105; c) M. Terrones, *Annu. Rev. Mater. Res.* **2003**, *33*, 419 – 501.
[19] a) H. J. Dai, *Acc. Chem. Res.* **2002**, *35*, 1035 – 1044; b) R. H. Baughman, A. A. Zakhidov, W. A. de Heer, *Science* **2002**, *297*, 787 – 792; c) E. Lamouroux, P. Serp, P. Kalck, *Catal. Rev.* **2007**, *49*, 341 – 405; d) E. Joselevich, H. J. Dai, J. Liu, K. Hata, A. H. Windle, *Top. Appl. Phys.* **2008**, *111*, 101 – 164; e) Q. Cao, J. A. Rogers, *Adv. Mater.* **2009**, *21*, 29 – 53; f) W. Y. Zhou, X. D. Bai, E. G. Wang, S. S. Xie, *Adv. Mater.* **2009**, *21*, 4565 – 4583; g) Z. F. Liu, L. Y. Jiao, Y. G. Yao, X. J. Xian, J. Zhang, *Adv. Mater.* **2010**, *22*, 2285 – 2310; h) Y. Li, R. L. Cui, L. Ding, Y. Liu, W. W. Zhou, Y. Zhang, Z. Jin, F. Peng, J. Liu, *Adv. Mater.* **2010**, *22*, 1508 – 1515; i) Y. N. Zhang, L. X. Zheng, *Nanoscale* **2010**, *2*, 1919 – 1929.
[20] a) C. Journet, P. Bernier, *Appl. Phys. A* **1998**, *67*, 1 – 9; b) R. Andrews, D. Jacques, D. L. Qian, T. Rantell, *Acc. Chem. Res.* **2002**, *35*, 1008 – 1017; c) K. Awasthi, A. Srivastava, O. N. Srivastava, *J. Nanosci. Nanotechnol.* **2005**, *5*, 1616 – 1636; d) C. H. See, A. T. Harris, *Ind. Eng. Chem. Res.* **2007**, *46*, 997 – 1012; e) R. Philippe, A. Moranqais, M. Corrias, B. Caussat, Y. Kihn, P. Kalck, D. Plee, P. Gaillard, D. Bernard, P. Serp, *Chem. Vap. Deposition* **2007**, *13*, 447 – 457; f) F. Danafar, A. Fakhru'l-Razi, M. A. M. Salleh, D. R. A. Biak, *Chem. Eng. J.* **2009**, *155*, 37 – 48; g) P. M. Ajayan, *Chem. Rev.* **1999**, *99*, 1787 – 1799; h) N. Grobert, *Mater. Today* **2007**, *10*, 28 – 35; i) C. Shen, A. H. Brozena, Y. H. Wang, *Nanoscale* **2011**, *3*, 503 – 518.
[21] F. Wei, Q. Zhang, W. Z. Qian, H. Yu, Y. Wang, G. H. Luo, G. H. Xu, D. Z. Wang, *Powder Technol.* **2008**, *183*, 10 – 20.
[22] a) A. V. Melechko, V. I. Merkulov, T. E. McKnight, M. A. Guillorn, K. L. Klein, D. H. Lowndes, M. L. Simpson, *J. Appl. Phys.* **2005**, *97*, 041301; b) H. Chen, A. Roy, B. J. B. , L. Zhu, J. Qu, L. M. Dai, *Mater. Sci. Eng. R* **2010**, *70*, 63 – 91; c) G. D. Nessim, *Nanoscale* **2010**, *2*, 1306 – 1323.
[23] M. Q. Zhao, Q. Zhang, X. L. Jia, J. Q. Huang, Y. H. Zhang, F. Wei, *Adv. Funct. Mater.* **2010**, *20*, 677 – 685.
[24] S. S. Fan, M. G. Chapline, N. R. Franklin, T. W. Tombler, A. M. Cassell, H. J. Dai, *Science* **1999**, *283*, 512 – 514.
[25] X. S. Wang, Q. Q. Li, J. Xie, Z. Jin, J. Y. Wang, Y. Li, K. L. Jiang, S. S. Fan, *Nano Lett.* **2009**, *9*, 3137 – 3141.
[26] T. W. Ebbesen, P. M. Ajayan, *Nature* **1992**, *358*, 220 – 222.
[27] T. Guo, P. Nikolaev, A. G. Rinzler, D. Tomanek, D. T. Colbert, R. E. Smalley, *J. Phys. Chem.* **1995**, *99*, 10694 – 10697.
[28] P. S. L. Schützenberger, *C. R. Acad. Sci.* **1890**, *111*, 774 – 778.
[29] a) D. Duprez, M. C. Demicheli, P. Marecot, J. Barbier, O. A. Ferretti, E. N. Ponzi, *J. Catal.* **1990**, *124*, 324 – 335; b) G. F. Froment, *Rev. Chem. Eng.* **1990**, *6*, 293 – 328; c) L. J. Velenyi, Y. H. Song, J. C. Fagley, *Ind. Eng. Chem. Res.* **1991**, *30*, 1708 – 1712; d) W. Q. Xu, Y. G. Yin, S. L. Suib, C. L. Oyoung, *J. Phys. Chem.* **1995**, *99*, 758 – 765; e) D. L. Trimm, *Catal. Today* **1997**, *37*, 233 – 238.
[30] a) R. T. K. Baker, M. A. Barber, R. J. Waite, P. S. Harris, F. S. Feates, *J. Catal.* **1972**, *26*, 51 – 62; b) R. T. K. Baker, P. S. Harris, R. B. Thomas, R. J. Waite, *J. Catal.* **1973**, *30*, 86 – 95; c) R. T. K. Baker, *Carbon* **1989**, *27*, 315 – 323; d) K. P. de Jong, J. W. Geus, *Catal. Rev.* **2000**, *42*, 481 – 510.
[31] M. José-Yacamán, M. Mikiyoshida, L. Rendon, J. G. Santiesteban, *Appl. Phys. Lett.* **1993**, *62*, 657 – 659.
[32] a) V. Ivanov, J. B. Nagy, P. Lambin, A. Lucas, X. B. Zhang, X. F. Zhang, D. Bernaerts, G. Vantendeloo, S. Amelinckx, J. Vanlanduyt, *Chem. Phys. Lett.* **1994**, *223*, 329 – 335; b) V. Ivanov, A. Fonseca, J. B. Nagy, A. Lucas, P. Lambin, D. Bernaerts, X. B. Zhang, *Carbon* **1995**, *33*, 1727 – 1738.
[33] K. Hernadi, A. Fonseca, J. B. Nagy, D. Bernaerts, A. A. Lucas, *Carbon* **1996**, *34*, 1249 – 1257.
[34] P. Chen, H. B. Zhang, G. D. Lin, Q. Hong, K. R. Tsai, *Carbon* **1997**, *35*, 1495 – 1501.
[35] I. Willems, Z. Konya, J. F. Colomer, G. Van Tendeloo, N. Nagaraju, A. Fonseca, J. B. Nagy, *Chem. Phys. Lett.* **2000**, *317*, 71 – 76.
[36] E. Flahaut, R. Bacsa, A. Peigney, C. Laurent, *Chem. Commun.* **2003**, 1442 – 1443.
[37] D. Venegoni, P. Serp, R. Feurer, Y. Kihn, C. Vahlas, P. Kalck, *Carbon* **2002**, *40*, 1799 – 1807.
[38] Y. Li, X. B. Zhang, X. Y. Tao, J. M. Xu, W. Z. Huang, J. H. Luo, Z. Q. Luo, T. Li, F. Liu, Y. Bao, H. J. Geise, *Carbon* **2005**, *43*, 295 – 301.
[39] F. Li, Q. Tan, D. G. Evans, X. Duan, *Catal. Lett.* **2005**, *99*, 151 – 156.
[40] A. Morancais, B. Caussat, Y. Kihn, P. Kalck, D. Plee, P. Gaillard, D. Bernard, P. Serp, *Carbon* **2007**, *45*, 624 – 635.
[41] Z. Wang, D. Z. Wang, L. J. Ji, J. J. Wu, R. Wang, J. Liang, *Chem. Vap. Deposition* **2006**, *12*, 417 – 419.
[42] S. P. Chai, S. H. S. Zein, A. R. Mohamed, *Appl. Catal. A* **2007**, *326*, 173 – 179.
[43] C. H. See, A. T. Harris, *AIChE J.* **2008**, *54*, 657 – 664.
[44] Z. X. Yu, D. Chen, M. Ronning, B. Totdal, T. Vralstad, E. Ochoa-Fernandez, A. Holmen, *Appl. Catal. A* **2008**, *338*, 147 – 158.
[45] X. K. Li, G. M. Yuan, A. Westwood, H. B. Zhang, Z. J. Dong, A. Brown, R. Brydson, B. Rand, *Chem. Vap. Deposition* **2008**, *14*, 40 – 45.
[46] S. Y. Son, Y. Lee, S. Won, D. H. Lee, S. D. Kim, S. W. Sung, *Ind. Eng. Chem. Res.* **2008**, *47*, 2166 – 2175.
[47] L. M. Cele, N. J. Coville, *Carbon* **2009**, *47*, 1824 – 1832.
[48] Y. Jia, L. F. He, L. T. Kong, J. Y. Liu, Z. Guo, F. L. Meng, T. Luo, M. Q. Li, J. H. Liu, *Carbon* **2009**, *47*, 1652 – 1658.
[49] K. Y. Tran, B. Heinrichs, J. F. Colomer, J. P. Pirard, S. Lambert, *Appl. Catal. A* **2007**, *318*, 63 – 69.
[50] C. T. Hsieh, Y. T. Lin, W. Y. Chen, J. L. Wei, *Powder Technol.* **2009**, *192*, 16 – 22.
[51] P. Landois, A. Peigney, C. Laurent, L. Frin, L. Datas, E. Flahaut, *Carbon* **2009**, *47*, 789 – 794.
[52] L. Zhang, F. Li, X. Xiang, M. Wei, D. G. Evans, *Chem. Eng. J.* **2009**, *155*, 474 – 482.
[53] R. Benito, M. Herrero, F. M. Labajos, V. Rives, C. Royo, N. Latorre, A. Monzon, *Chem. Eng. J.* **2009**, *149*, 455 – 462.
[54] V. Jimenez, A. Nieto-Marquez, J. A. Diaz, R. Romero, P. Sanchez, J. L. Valverde, A. Romero, *Ind. Eng. Chem. Res.* **2009**, *48*, 8407 – 8417.
[55] J. L. Song, L. Wang, S. A. Feng, J. H. Zhao, Z. P. Zhu, *New Carbon Mater.* **2009**, *24*, 307 – 313.
[56] J. Liu, A. T. Harris, *AIChE J.* **2010**, *56*, 102 – 113.
[57] O. M. Dunens, K. J. MacKenzie, A. T. Harris, *Ind. Eng. Chem. Res.* **2010**, *49*, 4031 – 4035.
[58] Y. Cao, Y. Zhao, Q. Z. Jiao, *Mater. Chem. Phys.* **2010**, *122*, 612 – 616.
[59] R. L. Xue, Z. P. Sun, L. H. Su, X. G. Zhang, *Catal. Lett.* **2010**, *135*, 312 – 320.
[60] C. N. He, N. Q. Zhao, C. S. Shi, S. Z. Song, *J. Alloys Compd.* **2010**, *489*, 20 – 25.
[61] J. P. Tessonnier, M. Becker, W. Xia, F. Girgsdies, R. Blume, L. D. Yao, D. S. Su, M. M. , R. Schlogl, *ChemCatChem* **2010**, *2*, 1559 – 1561.
[62] S. Iijima, T. Ichihashi, *Nature* **1993**, *363*, 603 – 605.
[63] D. S. Bethune, C. H. Kiang, M. S. Devries, G. Gorman, R. Savoy, J. Vazquez, R. Beyers, *Nature* **1993**, *363*, 605 – 607.
[64] H. J. Dai, A. G. Rinzler, P. Nikolaev, A. Thess, D. T. Colbert, R. E. Smalley, *Chem. Phys. Lett.* **1996**, *260*, 471 – 475.
[65] A. Thess, R. Lee, P. Nikolaev, H. J. Dai, P. Petit, J. Robert, C. H. Xu, Y. H. Lee, S. G. Kim, A. G. Rinzler, D. T. Colbert, G. E. Scuseria, D. Tomanek, J. E. Fischer, R. E. Smalley, *Science* **1996**, *273*, 483 – 487.
[66] C. Journet, W. K. Maser, P. Bernier, A. Loiseau, M. L. delaChapelle, S. Lefrant, P. Deniard, R. Lee, J. E. Fischer, *Nature* **1997**, *388*, 756 – 758.
[67] a) H. M. Cheng, F. Li, G. Su, H. Y. Pan, L. L. He, X. Sun, M. S. Dresselhaus, *Appl. Phys. Lett.* **1998**, *72*, 3282 – 3284; b) H. M. Cheng, F. Li, X. Sun, S. D. M. Brown, M. A. Pimenta, A. Marucci, G. Dresselhaus, M. S. Dresselhaus, *Chem. Phys. Lett.* **1998**, *289*, 602 – 610.
[68] J. Kong, A. M. Cassell, H. J. Dai, *Chem. Phys. Lett.* **1998**, *292*, 567 – 574.
[69] J. H. Hafner, M. J. Bronikowski, B. R. Azamian, P. Nikolaev, A. G. Rinzler, D. T. Colbert, K. A. Smith, R. E. Smalley, *Chem. Phys. Lett.* **1998**, *296*, 195 – 202.
[70] J. F. Colomer, C. Stephan, S. Lefrant, G. Van Tendeloo, I. Willems, Z. Konya, A. Fonseca, C. Laurent, J. B. Nagy, *Chem. Phys. Lett.* **2000**, *317*, 83 – 89.
[71] Q. W. Li, H. Yan, Y. Cheng, J. Zhang, Z. F. Liu, *J. Mater. Chem.* **2002**, *12*, 1179 – 1183.

[72] S. C. Lyu, B. C. Liu, S. H. Lee, C. Y. Park, H. K. Kang, C. W. Yang, C. J. Lee, *J. Phys. Chem. B* **2004**, *108*, 1613 – 1616.
[73] E. Lamouroux, P. Serp, Y. Kihn, P. Kalck, *Catal. Commun.* **2006**, *7*, 604 – 609.
[74] S. Maruyama, R. Kojima, Y. Miyauchi, S. Chiashi, M. Kohno, *Chem. Phys. Lett.* **2002**, *360*, 229 – 234.
[75] Y. L. Li, I. A. Kinloch, M. S. Shaffer, J. F. Geng, B. Johnson, A. H. Windle, *Chem. Phys. Lett.* **2004**, *384*, 98 – 102.
[76] A. J. Hart, A. H. Slocum, L. Royer, *Carbon* **2006**, *44*, 348 – 359.
[77] H. Yu, Q. Zhang, Q. F. Zhang, Q. X. Wang, G. Q. Ning, G. H. Luo, F. Wei, *Carbon* **2006**, *44*, 1706 – 1712.
[78] G. Q. Ning, F. Wei, Q. Wen, G. H. Luo, Y. Wang, Y. Jin, *J. Phys. Chem. B* **2006**, *110*, 1201 – 1205.
[79] Y. Zhao, Q. Z. Jiao, C. H. Li, J. Liang, *Carbon* **2007**, *45*, 2159 – 2163.
[80] Y. S. Chen, J. H. Huang, J. L. Hu, C. C. Yang, W. P. Kang, *Carbon* **2007**, *45*, 3007 – 3014.
[81] J. Q. Nie, W. Z. Qian, Q. Zhang, Q. Wen, F. Wei, *J. Phys. Chem. C* **2009**, *113*, 20178 – 20183.
[82] M. Q. Zhao, Q. Zhang, J. Q. Huang, J. Q. Nie, F. Wei, *Carbon* **2010**, *48*, 3260 – 3270.
[83] a) H. Z. Geng, K. K. Kim, K. Lee, G. Y. Kim, H. K. Choi, D. S. Lee, K. H. An, Y. H. Lee, Y. Chang, Y. S. Lee, B. Kim, Y. J. Lee, *Nano* **2007**, *2*, 157 – 167; b) E. M. Doherty, S. De, P. E. Lyons, A. Shmeliov, P. N. Nirmalraj, V. Scardaci, J. Joimel, W. J. Blau, J. J. Boland, J. N. Coleman, *Carbon* **2009**, *47*, 2466 – 2473.
[84] R. Sen, A. Govindaraj, C. N. R. Rao, *Chem. Mater.* **1997**, *9*, 2078 – 2081.
[85] M. Su, B. Zheng, J. Liu, *Chem. Phys. Lett.* **2000**, *322*, 321 – 326.
[86] a) B. Kitiyanan, W. E. Alvarez, J. H. Harwell, D. E. Resasco, *Chem. Phys. Lett.* **2000**, *317*, 497 – 503; b) J. E. Herrera, L. Balzano, A. Borgna, W. E. Alvarez, D. E. Resasco, *J. Catal.* **2001**, *204*, 129 – 145.
[87] H. Ago, S. Imamura, T. Okazaki, T. Saitoj, M. Yumura, M. Tsuji, *J. Phys. Chem. B* **2005**, *109*, 10035 – 10041.
[88] a) Y. Chen, B. Wang, L. J. Li, Y. H. Yang, D. Ciuparu, S. Y. Lim, G. L. Haller, L. D. Pfefferle, *Carbon* **2007**, *45*, 2217 – 2228; b) X. B. Liu, H. Sun, Y. Chen, R. Lau, Y. H. Yang, *Chem. Eng. J.* **2008**, *142*, 331 – 336; c) K. Kobayashi, R. Kitaura, Y. Kumai, Y. Goto, S. Inagaki, H. Shinohara, *Carbon* **2009**, *47*, 722 – 730.
[89] M. Q. Zhao, Q. Zhang, W. Zhang, J. Q. Huang, Y. H. Zhang, D. S. Su, F. Wei, *J. Am. Chem. Soc.* **2010**, *132*, 14739 – 14741.
[90] W. Z. Li, S. S. Xie, L. X. Qian, B. H. Chang, B. S. Zou, W. Y. Zhou, R. A. Zhao, G. Wang, *Science* **1996**, *274*, 1701 – 1703.
[91] M. Terrones, N. Grobert, J. Olivares, J. P. Zhang, H. Terrones, K. Kordatos, W. K. Hsu, J. P. Hare, P. D. Townsend, K. Prassides, A. K. Cheetham, H. W. Kroto, D. R. M. Walton, *Nature* **1997**, *388*, 52 – 55.
[92] Z. F. Ren, Z. P. Huang, J. W. Xu, J. H. Wang, P. Bush, M. P. Siegal, P. N. Provencio, *Science* **1998**, *282*, 1105 – 1107.
[93] R. Andrews, D. Jacques, A. M. Rao, F. Derbyshire, D. Qian, X. Fan, E. C. Dickey, J. Chen, *Chem. Phys. Lett.* **1999**, *303*, 467 – 474.
[94] S. M. Huang, L. M. Dai, A. W. H. Mau, *J. Phys. Chem. B* **1999**, *103*, 4223 – 4227.
[95] C. J. Lee, D. W. Kim, T. J. Lee, Y. C. Choi, Y. S. Park, Y. H. Lee, W. B. Choi, N. S. Lee, G. S. Park, J. M. Kim, *Chem. Phys. Lett.* **1999**, *312*, 461 – 468.
[96] B. C. Satishkumar, A. Govindaraj, C. N. R. Rao, *Chem. Phys. Lett.* **1999**, *307*, 158 – 162.
[97] Z. J. Zhang, B. Q. Wei, G. Ramanath, P. M. Ajayan, *Appl. Phys. Lett.* **2000**, *77*, 3764 – 3766.
[98] M. Mayne, N. Grobert, M. Terrones, R. Kamalakaran, M. Ruhle, H. W. Kroto, D. R. M. Walton, *Chem. Phys. Lett.* **2001**, *338*, 101 – 107.
[99] S. H. Jeong, O. J. Lee, K. H. Lee, S. H. Oh, C. G. Park, *Chem. Mater.* **2002**, *14*, 1859 – 1862.
[100] Y. Murakami, S. Chiashi, Y. Miyauchi, M. H. Hu, M. Ogura, T. Okubo, S. Maruyama, *Chem. Phys. Lett.* **2004**, *385*, 298 – 303.
[101] C. Singh, M. S. P. Shaffer, K. K. K. Koziol, I. A. Kinloch, A. H. Windle, *Chem. Phys. Lett.* **2003**, *372*, 860 – 865.
[102] G. F. Zhong, T. Iwasaki, K. Honda, Y. Furukawa, I. Ohdomari, H. Kawarada, *Chem. Vap. Deposition* **2005**, *11*, 127 – 130.
[103] A. J. Hart, A. H. Slocum, *J. Phys. Chem. B* **2006**, *110*, 8250 – 8257.
[104] A. Barreiro, D. Selbmann, T. Pichler, K. Biedermann, T. Gemming, M. H. Rummeli, U. Schwalke, B. Buchner, *Appl. Phys. A* **2006**, *82*, 719 – 725.
[105] L. Zhang, Z. R. Li, Y. Q. Tan, G. Lolli, N. Sakulchaicharoen, F. G. Requejo, B. S. Mun, D. E. Resasco, *Chem. Mater.* **2006**, *18*, 5624 – 5629.
[106] W. H. Wang, T. H. Hong, C. T. Kuo, *Carbon* **2007**, *45*, 97 – 102.
[107] I. Gunjishima, T. Inoue, S. Yamamuro, K. Sumiyama, A. Okamoto, *Carbon* **2007**, *45*, 1193 – 1199.
[108] J. Y. Qu, Z. B. Zhao, J. S. Qiu, Y. Gogotsi, *Chem. Commun.* **2008**, 2747 – 2749.
[109] L. T. Qu, F. Du, L. M. Dai, *Nano Lett.* **2008**, *8*, 2682 – 2687.
[110] C. L. Pint, N. Nicholas, S. T. Pheasant, J. G. Duque, A. Nicholas, G. Parra-Vasquez, G. Eres, M. Pasquali, R. H. Hauge, *J. Phys. Chem. C* **2008**, *112*, 14041 – 14051.
[111] G. D. Nessim, A. J. Hart, J. S. Kim, D. Acquaviva, J. H. Oh, C. D. Morgan, M. Seita, J. S. Leib, C. V. Thompson, *Nano Lett.* **2008**, *8*, 3587 – 3593.
[112] a) X. W. Cui, W. F. Wei, C. Harrower, W. X. Chen, *Carbon* **2009**, *47*, 3441 – 3451; b) X. W. Cui, W. F. Wei, W. X. Chen, *Carbon* **2010**, *48*, 2782 – 2791.
[113] Q. Zhang, M. Q. Zhao, J. Q. Huang, J. Q. Nie, F. Wei, *Carbon* **2010**, *48*, 1196 – 1209.
[114] H. Sugime, S. Noda, *Carbon* **2010**, *48*, 2203 – 2211.
[115] P. M. Ajayan, O. Stephan, C. Colliex, D. Trauth, *Science* **1994**, *265*, 1212 – 1214.
[116] a) W. A. Deheer, W. S. Bacsa, A. Chatelain, T. Gerfin, R. Humphreybaker, L. Forro, D. Ugarte, *Science* **1995**, *268*, 845 – 847; b) D. A. Walters, M. J. Casavant, X. C. Qin, C. B. Huffman, P. J. Boul, L. M. Ericson, E. H. Haroz, M. J. O'Connell, K. Smith, D. T. Colbert, R. E. Smalley, *Chem. Phys. Lett.* **2001**, *338*, 14 – 20.
[117] B. Vigolo, A. Penicaud, C. Coulon, C. Sauder, R. Pailler, C. Journet, P. Bernier, P. Poulin, *Science* **2000**, *290*, 1331 – 1334.
[118] B. Wang, Y. F. Ma, N. Li, Y. P. Wu, F. F. Li, Y. S. Chen, *Adv. Mater.* **2010**, *22*, 3067 – 3070.
[119] Z. W. Pan, S. S. Xie, B. H. Chang, C. Y. Wang, L. Lu, W. Liu, M. Y. Zhou, W. Z. Li, *Nature* **1998**, *394*, 631 – 632.
[120] a) Z. H. Wen, Q. Wang, J. H. Li, *Adv. Funct. Mater.* **2008**, *18*, 959 – 964; b) W. C. Tsai, S. J. Wang, J. K. Lin, C. L. Chang, R. M. Ko, *Electrochem. Commun.* **2009**, *11*, 660 – 663; c) Y. H. Yan, M. B. Chan-Park, Q. Zhang, *Small* **2007**, *3*, 24 – 42.
[121] a) R. Sen, A. Govindaraj, C. N. R. Rao, *Chem. Phys. Lett.* **1997**, *267*, 276 – 280; b) C. N. R. Rao, R. Sen, B. C. Satishkumar, A. Govindaraj, *Chem. Commun.* **1998**, 1525 – 1526.
[122] B. Q. Wei, R. Vajtai, Y. Jung, J. Ward, R. Zhang, G. Ramanath, P. M. Ajayan, *Nature* **2002**, *416*, 495 – 496.
[123] S. G. Rao, L. Huang, W. Setyawan, S. H. Hong, *Nature* **2003**, *425*, 36 – 37.
[124] a) J. E. Fischer, W. Zhou, J. Vavro, M. C. Llaguno, C. Guthy, R. Haggenmueller, M. J. Casavant, D. E. Walters, R. E. Smalley, *J. Appl. Phys.* **2003**, *93*, 2157 – 2163; b) S. M. Jung, H. Y. Jung, J. S. Suh, *Carbon* **2008**, *46*, 1973 – 1977.
[125] X. L. Li, L. Zhang, X. R. Wang, I. Shimoyama, X. M. Sun, W. S. Seo, H. J. Dai, *J. Am. Chem. Soc.* **2007**, *129*, 4890 – 4891.
[126] Y. G. Zhang, A. L. Chang, J. Cao, Q. Wang, W. Kim, Y. M. Li, N. Morris, E. Yenilmez, J. Kong, H. J. Dai, *Appl. Phys. Lett.* **2001**, *79*, 3155 – 3157.
[127] E. Joselevich, C. M. Lieber, *Nano Lett.* **2002**, *2*, 1137 – 1141.
[128] S. M. Huang, X. Y. Cai, C. S. Du, J. Liu, *J. Phys. Chem. B* **2003**, *107*, 13251 – 13254.
[129] a) S. M. Huang, X. Y. Cai, J. Liu, *J. Am. Chem. Soc.* **2003**, *125*, 5636 – 5637; b) S. M. Huang, B. Maynor, X. Y. Cai, J. Liu, *Adv. Mater.* **2003**, *15*, 1651 – 1655.
[130] L. X. Zheng, M. J. O'Connell, S. K. Doorn, X. Z. Liao, Y. H. Zhao, E. A. Akhadov, M. A. Hoffbauer, B. J. Roop, Q. X. Jia, R. C. Dye, D. E. Peterson, S. M. Huang, J. Liu, Y. T. Zhu, *Nat. Mater.* **2004**, *3*, 673 – 676.
[131] C. Kocabas, M. A. Meitl, A. Gaur, M. Shim, J. A. Rogers, *Nano Lett.* **2004**, *4*, 2421 – 2426.
[132] a) S. D. Li, Z. Yu, C. Rutherglen, P. J. Burke, *Nano Lett.* **2004**, *4*, 2003 – 2007; b) Z. Yu, S. D. Li, P. J. Burke, *Chem. Mater.* **2004**, *16*, 3414 – 3416.
[133] A. Ismach, L. Segev, E. Wachtel, E. Joselevich, *Angew. Chem.* **2004**, *116*, 6266 – 6269; *Angew. Chem. Int. Ed.* **2004**, *43*, 6140 – 6143.
[134] S. Han, X. L. Liu, C. W. Zhou, *J. Am. Chem. Soc.* **2005**, *127*, 5294 – 5295.
[135] X. L. Liu, K. Ryu, A. Badmaev, S. Han, C. W. Zhou, *J. Phys. Chem. C* **2008**, *112*, 15929 – 15933.
[136] a) L. M. Huang, X. D. Cui, B. White, S. P. O'Brien, *J. Phys. Chem. B* **2004**, *108*, 16451 – 16456; b) L. M. Huang, B. White, M. Y. Sfeir, M. Y. Huang, H. X. Huang, S. Wind, J. Hone, S. O'Brien, *J. Phys. Chem. B* **2006**, *110*, 11103 – 11109.
[137] N. Kumar, W. Curtis, J. I. Hahm, *Appl. Phys. Lett.* **2005**, *86*, 173101.

[138] B. H. Hong, J. Y. Lee, T. Beetz, Y. M. Zhu, P. Kim, K. S. Kim, *J. Am. Chem. Soc.* **2005**, *127*, 15336 – 15337.

[139] A. Ismach, D. Kantorovich, E. Joselevich, *J. Am. Chem. Soc.* **2005**, *127*, 11554 – 11555.

[140] W. W. Zhou, Z. Y. Han, J. Y. Wang, Y. Zhang, Z. Jin, X. Sun, Y. W. Zhang, C. H. Yan, Y. Li, *Nano Lett.* **2006**, *6*, 2987 – 2990.

[141] a) H. Ago, K. Nakamura, K. Ikeda, N. Uehara, N. Ishigami, M. Tsuji, *Chem. Phys. Lett.* **2005**, *408*, 433 – 438; b) H. Ago, N. Uehara, K. Ikeda, R. Ohdo, K. Nakamura, M. Tsuji, *Chem. Phys. Lett.* **2006**, *421*, 399 – 403.

[142] A. Reina, M. Hofmann, D. Zhu, J. Kong, *J. Phys. Chem. C* **2007**, *111*, 7292 – 7297.

[143] C. Kocabas, N. Pimparkar, O. Yesilyurt, S. J. Kang, M. A. Alam, J. A. Rogers, *Nano Lett.* **2007**, *7*, 1195 – 1202.

[144] Y. G. Yao, Q. W. Li, J. Zhang, R. Liu, L. Y. Jiao, Y. T. Zhu, Z. F. Liu, *Nat. Mater.* **2007**, *6*, 283 – 286.

[145] K. M. Ryu, A. Badmaev, L. Gomez, F. Ishikawa, B. Lei, C. W. Zhou, *J. Am. Chem. Soc.* **2007**, *129*, 10104 – 10105.

[146] L. Ding, A. Tselev, J. Y. Wang, D. N. Yuan, H. B. Chu, T. P. McNicholas, Y. Li, J. Liu, *Nano Lett.* **2009**, *9*, 800 – 805.

[147] Y. G. Yao, C. Q. Feng, J. Zhang, Z. F. Liu, *Nano Lett.* **2009**, *9*, 1673 – 1677.

[148] G. Hong, B. Zhang, B. H. Peng, J. Zhang, W. M. Choi, J. Y. Choi, J. M. Kim, Z. F. Liu, *J. Am. Chem. Soc.* **2009**, *131*, 14642 – 14643.

[149] S. M. Huang, Q. R. Cai, J. Y. Chen, Y. Qian, L. J. Zhang, *J. Am. Chem. Soc.* **2009**, *131*, 2094 – 2095.

[150] N. Ishigami, H. Ago, K. Imamoto, M. Tsuji, K. Iakoubovskii, N. Minami, *J. Am. Chem. Soc.* **2008**, *130*, 9918 – 9924.

[151] Q. Wen, W. Z. Qian, J. Q. Nie, A. Y. Cao, G. Q. Ning, Y. Wang, L. Hu, Q. Zhang, J. Q. Huang, F. Wei, *Adv. Mater.* **2010**, *22*, 1867 – 1871.

[152] A. Rutkowska, D. Walker, S. Gorfman, P. A. Thomas, J. V. Macpherson, *J. Phys. Chem. C* **2009**, *113*, 17087 – 17096.

[153] S. W. Hong, T. Banks, J. A. Rogers, *Adv. Mater.* **2010**, *22*, 1826 – 1830.

[154] Y. Qian, C. Y. Wang, B. Huang, *Nanoscale Res. Lett.* **2010**, *5*, 442 – 447.

[155] Q. Wen, R. F. Zhang, W. Z. Qian, Y. R. Wang, P. H. Tan, J. Q. Nie, F. Wei, *Chem. Mater.* **2010**, *22*, 1294 – 1296.

[156] K. H. Lee, J. M. Cho, W. Sigmund, *Appl. Phys. Lett.* **2003**, *82*, 448 – 450.

[157] S. M. Huang, M. Woodson, R. Smalley, J. Liu, *Nano Lett.* **2004**, *4*, 1025 – 1028.

[158] a) B. L. Liu, W. C. Ren, L. B. Gao, S. S. Li, S. F. Pei, C. Liu, C. B. Jiang, H. M. Cheng, *J. Am. Chem. Soc.* **2009**, *131*, 2082 – 2083; b) S. A. Steiner, T. F. Baumann, B. C. Bayer, R. Blume, M. A. Worsley, W. J. MoberlyChan, E. L. Shaw, R. Schlogl, A. J. Hart, S. Hofmann, B. L. Wardle, *J. Am. Chem. Soc.* **2009**, *131*, 12144 – 12154; c) D. Takagi, Y. Kobayashi, Y. Hommam, *J. Am. Chem. Soc.* **2009**, *131*, 6922 – 6923; d) D. Takagi, H. Hibino, S. Suzuki, Y. Kobayashi, Y. Homma, *Nano Lett.* **2007**, *7*, 2272 – 2275; e) D. S. Yu, Q. Zhang, L. M. Dai, *J. Am. Chem. Soc.* **2010**, *132*, 15127 – 15129; f) B. L. Liu, D. M. Tang, C. H. Sun, C. Liu, W. C. Ren, F. Li, W. J. Yu, L. C. Yin, L. L. Zhang, C. B. Jiang, H. M. Cheng, *J. Am. Chem. Soc.* **2011**, *133*, 197 – 199.

[159] S. Helveg, C. Lopez-Cartes, J. Sehested, P. L. Hansen, B. S. Clausen, J. R. Rostrup-Nielsen, F. Abild-Pedersen, J. K. Norskov, *Nature* **2004**, *427*, 426 – 429.

[160] S. Yasuda, T. Hiraoka, D. N. Futaba, T. Yamada, M. Yumura, K. Hata, *Nano Lett.* **2009**, *9*, 769 – 773.

[161] R. S. Wagner, W. C. Ellis, *Appl. Phys. Lett.* **1964**, *4*, 89 – 90.

[162] Y. M. Li, W. Kim, Y. G. Zhang, M. Rolandi, D. W. Wang, H. J. Dai, *J. Phys. Chem. B* **2001**, *105*, 11424 – 11431.

[163] A. G. Nasibulin, P. V. Pikhitsa, H. Jiang, E. I. Kauppinen, *Carbon* **2005**, *43*, 2251 – 2257.

[164] Q. Zhang, M. Q. Zhao, J. Q. Huang, W. Z. Qian, F. Wei, *Chin. J. Catal.* **2008**, *29*, 1138 – 1144.

[165] a) R. Seidel, G. S. Duesberg, E. Unger, A. P. Graham, M. Liebau, F. Kreupl, *J. Phys. Chem. B* **2004**, *108*, 1888 – 1893; b) F. Ding, A. Rosen, K. Bolton, *Carbon* **2005**, *43*, 2215 – 2217.

[166] a) W. Z. Qian, T. Liu, F. Wei, Z. W. Wang, D. Z. Wang, Y. D. Li, *Carbon* **2003**, *41*, 2683 – 2686; b) W. Z. Qian, F. Wei, T. Liu, Z. W. Wang, Y. D. Li, *J. Chem. Phys.* **2003**, *118*, 878 – 882.

[167] a) R. T. Lv, F. Y. Kang, W. X. Wang, J. Q. Wei, J. L. Gu, K. L. Wang, D. H. Wu, *Carbon* **2007**, *45*, 1433 – 1438; b) R. T. Lv, F. Y. Kang, J. L. Gu, K. L. Wang, D. H. Wu, *Sci. China Technol. Sci.* **2010**, *53*, 1453 – 1459.

[168] H. Tobias, A. Soffer, *Carbon* **1985**, *23*, 281 – 289.

[169] a) Q. Zhang, H. Yu, J. Q. Huang, L. Hu, W. Z. Qian, D. Z. Wang, F. Wei, *Mater. Lett.* **2008**, *62*, 3149 – 3151; b) R. T. Lv, F. Y. Kang, D. Zhu, Y. Q. Zhu, X. C. Gui, J. Q. Wei, J. L. Gu, D. J. Li, K. L. Wang, D. H. Wu, *Carbon* **2009**, *47*, 2709 – 2715.

[170] a) X. L. Pan, Z. L. Fan, W. Chen, Y. J. Ding, H. Y. Luo, X. H. Bao, *Nat. Mater.* **2007**, *6*, 507 – 511; b) Y. S. Hu, X. Liu, J. O. Muller, R. Schlogl, J. Maier, D. S. Su, *Angew. Chem.* **2009**, *121*, 216 – 220; *Angew. Chem. Int. Ed.* **2009**, *48*, 210 – 214; c) D. S. Su, R. Schlögl, *ChemSusChem* **2010**, *3*, 136 – 168; d) D. S. Su, J. Zhang, B. Frank, A. Thomas, X. C. Wang, J. Paraknowitsch, R. Schlogl, *ChemSusChem* **2010**, *3*, 169 – 180.

[171] S. Reich, L. Li, J. Robertson, *Chem. Phys. Lett.* **2006**, *421*, 469 – 472.

[172] W. M. Zhu, A. Borjesson, K. Bolton, *Carbon* **2010**, *48*, 470 – 478.

[173] D. A. Gomez-Gualdron, P. B. Balbuena, *J. Phys. Chem. C* **2009**, *113*, 698 – 709.

[174] S. Hofmann, R. Sharma, C. Ducati, G. Du, C. Mattevi, C. Cepek, M. Cantoro, S. Pisana, A. Parvez, F. Cervantes-Sodi, A. C. Ferrari, R. Dunin-Borkowski, S. Lizzit, L. Petaccia, A. Goldoni, J. Robertson, *Nano Lett.* **2007**, *7*, 602 – 608.

[175] F. Ding, K. Bolton, A. Rosen, *J. Phys. Chem. B* **2004**, *108*, 17369 – 17377.

[176] F. Ding, A. R. Harutyunyan, B. I. Yakobson, *Proc. Natl. Acad. Sci. USA* **2009**, *106*, 2506 – 2509.

[177] M. Marchand, C. Journet, D. Guillot, J. M. Benoit, B. I. Yakobson, S. T. Purcell, *Nano Lett.* **2009**, *9*, 2961 – 2966.

[178] Q. Wang, M. F. Ng, S. W. Yang, Y. H. Yang, Y. A. Chen, *ACS Nano* **2010**, *4*, 939 – 946.

[179] M. S. Arnold, A. A. Green, J. F. Hulvat, S. I. Stupp, M. C. Hersam, *Nat. Nanotechnol.* **2006**, *1*, 60 – 65.

[180] a) A. A. Green, M. C. Hersam, *Nat. Nanotechnol.* **2009**, *4*, 64 – 70; b) M. C. Hersam, *Nat. Nanotechnol.* **2008**, *3*, 387 – 394.

[181] a) L. Wei, B. Wang, T. H. Goh, L. J. Li, Y. H. Yang, M. B. Chan-Park, Y. Chen, *J. Phys. Chem. B* **2008**, *112*, 2771 – 2774; b) P. Zhao, E. Einarsson, R. Xiang, Y. Murakami, S. Maruyama, *J. Phys. Chem. C* **2010**, *114*, 4831 – 4834; c) L. Y. Yan, W. F. Li, X. F. Fan, L. Wei, Y. Chen, J. L. Kuo, L. J. Li, S. K. Kwak, Y. G. Mu, M. B. Chan-Park, *Small* **2010**, *6*, 110 – 118; d) M. Zheng, A. Jagota, M. S. Strano, A. P. Santos, P. Barone, S. G. Chou, B. A. Diner, M. S. Dresselhaus, R. S. McLean, G. B. Onoa, G. G. Samsonidze, E. D. Semke, M. Usrey, D. J. Walls, *Science* **2003**, *302*, 1545 – 1548.

[182] H. L. Zhang, Y. Q. Liu, L. C. Cao, D. C. Wei, Y. Wang, H. Kajiura, Y. M. Li, K. Noda, G. F. Luo, L. Wang, J. Zhou, J. Lu, Z. X. Gao, *Adv. Mater.* **2009**, *21*, 813 – 816.

[183] D. C. Wei, Y. Q. Liu, L. C. Cao, H. L. Zhang, L. P. Huang, G. Yu, H. Kajiura, Y. M. Li, *Adv. Funct. Mater.* **2009**, *19*, 3618 – 3624.

[184] X. L. Li, X. M. Tu, S. Zaric, K. Welsher, W. S. Seo, W. Zhao, H. J. Dai, *J. Am. Chem. Soc.* **2007**, *129*, 15770 – 15771.

[185] M. He, A. I. Chernov, P. V. Fedotov, E. D. Obraztsova, J. Sainio, E. Rikkinen, H. Jiang, Z. Zhu, Y. Tian, E. I. Kauppinen, M. Niemela, A. O. I. Krauset, *J. Am. Chem. Soc.* **2010**, *132*, 13994 – 13996.

[186] Y. Hao, Q. F. Zhang, F. Wei, W. Z. Qian, G. H. Luo, *Carbon* **2003**, *41*, 2855 – 2863.

[187] W. Z. Qian, T. Liu, F. Wei, Z. W. Wang, G. H. Luo, H. Yu, Z. F. Li, *Carbon* **2003**, *41*, 2613 – 2617.

[188] a) Y. Wang, G. S. Gu, F. Wei, J. Wu, *Powder Technol.* **2002**, *124*, 152 – 159; b) Y. Wang, F. Wei, G. S. Gu, H. Yu, *Physica B* **2002**, *323*, 327 – 329.

[189] Y. Liu, W. Z. Qian, Q. Zhang, G. Q. Ning, Q. Wen, G. H. Luo, F. Wei, *Carbon* **2008**, *46*, 1860 – 1868.

[190] Q. Zhang, W. Z. Qian, Q. Wen, Y. Liu, D. H. Wang, F. Wei, *Carbon* **2007**, *45*, 1645 – 1650.

[191] Q. Wen, W. Z. Qian, F. Wei, Y. Liu, G. Q. Ning, Q. Zhang, *Chem. Mater.* **2007**, *19*, 1226 – 1230.

[192] a) L. J. Ci, Z. L. Rao, Z. P. Zhou, D. S. Tang, Y. Q. Yan, Y. X. Liang, D. F. Liu, H. J. Yuan, W. Y. Zhou, G. Wang, W. Liu, S. S. Xie, *Chem. Phys. Lett.* **2002**, *359*, 63 – 67; b) J. Q. Wei, L. J. Ci, B. Jiang, Y. H. Li, X. F. Zhang, H. W. Zhu, C. L. Xu, D. H. Wu, *J. Mater. Chem.* **2003**, *13*, 1340 – 1344; c) Z. P. Zhou, L. J. Ci, L. Song, X. Q. Yan, D. F. Liu, H. J. Yuan, Y. Gao, J. X. Wang, L. F. Liu, W. Y. Zhou, G. Wang, S. S. Xie, *Carbon* **2003**, *41*, 2607 – 2611.

[193] a) H. W. Zhu, C. L. Xu, D. H. Wu, B. Q. Wei, R. Vajtai, P. M. Ajayan, *Science* **2002**, *296*, 884 – 886; b) J. J. Vilatela, A. H. Windle, *Adv. Mater.* **2010**, *22*, 4959 – 4963.

[194] J. H. Luo, X. B. Zhang, Y. Li, J. P. Chen, F. Liu, *J. Inorg. Mater.* **2005**, *20*, 1358 – 1362.

[195] L. Liu, S. S. Fan, *J. Am. Chem. Soc.* **2001**, *123*, 11502 – 11503.

[196] X. S. Li, A. Y. Cao, Y. J. Jung, R. Vajtai, P. M. Ajayan, *Nano Lett.* **2005**, *5*, 1997 – 2000.
[197] L. B. Zhu, D. W. Hess, C. P. Wong, *J. Phys. Chem. B* **2006**, *110*, 5445 – 5449.
[198] L. B. Zhu, J. W. Xu, F. Xiao, H. J. Jiang, D. W. Hess, C. P. Wong, *Carbon* **2007**, *45*, 344 – 348.
[199] Q. Zhang, W. P. Zhou, W. Z. Qian, R. Xiang, J. Q. Huang, D. Z. Wang, F. Wei, *J. Phys. Chem. C* **2007**, *111*, 14638 – 14643.
[200] R. Xiang, G. H. Luo, W. Z. Qian, Q. Zhang, Y. Wang, F. Wei, Q. Li, A. Y. Cao, *Adv. Mater.* **2007**, *19*, 2360 – 2363.
[201] A. J. Hart, A. H. Slocum, *Nano Lett.* **2006**, *6*, 1254 – 1260.
[202] J. Q. Huang, Q. Zhang, G. H. Xu, W. Z. Qian, F. Wei, *Nanotechnology* **2008**, *19*, 435602.
[203] R. Xiang, G. Luo, W. Qian, Y. Wang, F. Wei, Q. Li, *Chem. Vap. Deposition* **2007**, *13*, 533 – 536.
[204] Q. Zhang, J. Q. Huang, F. Wei, G. H. Xu, Y. Wang, W. Z. Qian, D. Z. Wang, *Chin. Sci. Bull.* **2007**, *52*, 2896 – 2902.
[205] Q. Zhang, J. Q. Huang, M. Q. Zhao, W. Z. Qian, Y. Wang, F. Wei, *Carbon* **2008**, *46*, 1152 – 1158.
[206] a) N. Yamamoto, A. J. Hart, E. J. Garcia, S. S. Wicks, H. M. Duong, A. H. Slocum, B. L. Wardle, *Carbon* **2009**, *47*, 551 – 560; b) A. Y. Cao, V. P. Veedu, X. S. Li, Z. L. Yao, M. N. Ghasemi-Nejhad, P. M. Ajayan, *Nat. Mater.* **2005**, *4*, 540 – 545; c) Q. Zhang, W. Z. Qian, R. Xiang, Z. Yang, G. H. Luo, Y. Wang, F. Wei, *Mater. Chem. Phys.* **2008**, *107*, 317 – 321; d) H. Qian, A. Bismarck, E. S. Greenhalgh, M. S. P. Shaffer, *Carbon* **2010**, *48*, 277 – 286; e) H. Qian, E. S. Greenhalgh, M. S. P. Shaffer, A. Bismarck, *J. Mater. Chem.* **2010**, *20*, 4751 – 4762; f) K. Zhou, J. Q. Huang, Q. Zhang, F. Wei, *Nanoscale Res. Lett.* **2010**, *5*, 1555 – 1560.
[207] a) C. L. Pint, S. T. Pheasant, M. Pasquali, K. E. Coulter, H. K. Schmidt, R. H. Hauge, *Nano Lett.* **2008**, *8*, 1879 – 1883; b) C. L. Pint, N. T. Alvarez, R. H. Hauge, *Nano Res.* **2009**, *2*, 526 – 534; c) N. T. Alvarez, C. E. Hamilton, C. L. Pint, A. Orbaek, J. Yao, A. L. Frosinini, A. R. Barron, J. M. Tour, R. H. Hauge, *ACS Appl. Mater. Interfaces* **2010**, *2*, 1851 – 1856; d) M. Q. Zhao, J. Q. Huang, Q. Zhang, J. Q. Nie, F. Wei, *Carbon* **2011**, *49*, 2148 – 2152.
[208] Q. Zhang, M. Q. Zhao, D. M. Tang, F. Li, J. Q. Huang, B. L. Liu, W. C. Zhu, Y. H. Zhang, F. Wei, *Angew. Chem.* **2010**, *122*, 3724 – 3727; *Angew. Chem. Int. Ed.* **2010**, *49*, 3642 – 3645.
[209] a) D. L. He, M. Bozlar, M. Genestoux, J. B. Bai, *Carbon* **2010**, *48*, 1159 – 1170; b) D. L. He, H. Li, W. L. Li, P. Haghi-Ashtiani, P. L. , J. B. Bai, *Carbon* **2011**, *49*, 2273 – 2286; c) D. Y. Kim, H. Sugime, K. Hesegawa, T. Osawa, S. Noda, *Carbon* **2011**, *49*, 1972 – 1979; d) R. Philippe, B. Caussat, A. Falqui, Y. Kihn, P. Kalck, S. Bordere, D. Plee, P. Gaillard, D. Bernard, P. Serp, *J. Catal.* **2009**, *263*, 345 – 358.
[210] Q. Zhang, M. Q. Zhao, Y. Liu, A. Y. Cao, W. Z. Qian, Y. F. Lu, F. Wei, *Adv. Mater.* **2009**, *21*, 2876 – 2880.
[211] D. Geldart, *Powder Technol.* **1973**, *7*, 285 – 292.
[212] a) Q. Zhang, M. Q. Zhao, J. Q. Huang, Y. Liu, Y. Wang, W. Z. Qian, F. Wei, *Carbon* **2009**, *47*, 2600 – 2610; b) M. Q. Zhao, Q. Zhang, J. Q. Huang, F. Wei, *J. Phys. Chem. Solids* **2010**, *71*, 624 – 626.
[213] a) T. F. Wang, J. F. Wang, Y. Jin, *Ind. Eng. Chem. Res.* **2007**, *46*, 5824 – 5847; b) Y. Cheng, C. N. Wu, J. X. Zhu, F. Wei, Y. Jin, *Powder Technol.* **2008**, *183*, 364 – 384.
[214] M. P. Dudukovic, *Chem. Eng. Sci.* **2010**, *65*, 3 – 11.
[215] W. Z. Qian, F. Wei, Z. W. Wang, T. Liu, H. Yu, G. H. Luo, L. Xiang, X. Y. Deng, *AIChE J.* **2003**, *49*, 619 – 625.
[216] Q. Zhang, M. Q. Zhao, J. Q. Huang, F. Wei, *Powder Technol.* **2010**, *198*, 285 – 291.
[217] H. Yu, Q. F. Zhang, G. S. Gu, Y. Wang, G. H. Luo, F. Wei, *AIChE J.* **2006**, *52*, 4110 – 4123.
[218] L. Ni, K. Kuroda, L. P. Zhou, T. Kizuka, K. Ohta, K. Matsuishi, J. Nakamura, *Carbon* **2006**, *44*, 2265 – 2272.
[219] S. L. Pirard, S. Douven, C. Bossuot, G. Heyen, J. P. Pirard, *Carbon* **2007**, *45*, 1167 – 1175.
[220] R. Philippe, P. Serp, P. Kalck, Y. Kihn, S. Bordere, D. Plee, P. Gaillard, D. Bernard, B. Caussat, *AIChE J.* **2009**, *55*, 450 – 464.
[221] R. Philippe, P. Serp, P. Kalck, S. Bordere, D. Plee, P. Gaillard, D. Bernard, B. Caussat, *AIChE J.* **2009**, *55*, 465 – 474.
[222] a) A. J. Hart, L. van Laake, A. H. Slocum, *Small* **2007**, *3*, 772 – 777; b) A. A. Puretzky, D. B. Geohegan, S. Jesse, I. N. Ivanov, G. Eres, *Appl. Phys. A* **2005**, *81*, 223 – 240; c) J. Q. Huang, Q. Zhang, M. Q. Zhao, K. Zhou, F. Wei, *Carbon* **2011**, *49*, 1395 – 1400.
[223] E. Einarsson, Y. Murakami, M. Kadowaki, S. Maruyama, *Carbon* **2008**, *46*, 923 – 930.
[224] K. Liu, K. L. Jiang, C. Feng, Z. Chen, S. S. Fan, *Carbon* **2005**, *43*, 2850 – 2856.
[225] G. F. Zhong, T. Iwasaki, J. Robertson, H. Kawarada, *J. Phys. Chem. B* **2007**, *111*, 1907 – 1910.
[226] a) X. F. Zhang, A. Y. Cao, B. Q. Wei, Y. H. Li, J. Q. Wei, C. L. Xu, D. H. Wu, *Chem. Phys. Lett.* **2002**, *362*, 285 – 290; b) Z. Yang, Q. Zhang, G. H. Luo, R. Xiang, W. Z. Qan, Y. Wang, F. Wei, *New Carbon Mater.* **2010**, *25*, 168 – 174.
[227] J. M. Ting, W. Y. Wu, K. H. Liao, H. H. Wu, *Carbon* **2009**, *47*, 2671 – 2678.
[228] R. Xiang, Z. Yang, Q. Zhang, G. H. Luo, W. Z. Qian, F. Wei, M. Kadowaki, E. Einarsson, S. Maruyama, *J. Phys. Chem. C* **2008**, *112*, 4892 – 4896.
[229] a) D. N. Futaba, K. Hata, T. Yamada, K. Mizuno, M. Yumura, S. Iijima, *Phys. Rev. Lett.* **2005**, *95*, 056104; b) K. Bosnick, L. Dai, *J. Phys. Chem. C* **2010**, *114*, 7226 – 7230.
[230] a) Y. T. Lee, J. Park, Y. S. Choi, H. Ryu, H. J. Lee, *J. Phys. Chem. B* **2002**, *106*, 7614 – 7618; b) K. E. Kim, K. J. Kim, W. S. Jung, S. Y. Bae, J. Park, J. Choi, J. Choo, *Chem. Phys. Lett.* **2005**, *401*, 459 – 464; c) M. J. Bronikowski, *J. Phys. Chem. C* **2007**, *111*, 17705 – 17712.
[231] C. T. Wirth, C. Zhang, G. F. Zhong, S. Hofmann, J. Robertson, *ACS Nano* **2009**, *3*, 3560 – 3566.
[232] a) X. S. Li, L. Ci, S. Kar, C. Soldano, S. J. Kilpatrick, P. M. Ajayan, *Carbon* **2007**, *45*, 847 – 851; b) X. F. Feng, K. Liu, X. Xie, R. F. Zhou, L. N. Zhang, Q. Q. Li, S. S. Fan, K. L. Jiang, *J. Phys. Chem. C* **2009**, *113*, 9623 – 9631.
[233] E. R. Meshot, A. J. Hart, *Appl. Phys. Lett.* **2008**, *92*, 113107.
[234] M. Bedewy, E. R. Meshot, H. C. Guo, E. A. Verploegen, W. Lu, A. J. Hart, *J. Phys. Chem. C* **2009**, *113*, 20576 – 20582.
[235] S. M. Kim, C. L. Pint, P. B. Amama, D. N. Zakharov, R. H. Hauge, B. Maruyama, E. A. Stach, *J. Phys. Chem. Lett.* **2010**, *1*, 918 – 922.
[236] E. R. Meshot, M. Bedewy, K. M. Lyons, A. R. Woll, K. A. Juggernauth, S. Tawfick, A. J. Hart, *Nanoscale* **2010**, *2*, 896 – 900.
[237] A. E. Agboola, R. W. Pike, T. A. Hertwig, H. H. Lou, *Clean Technol. Environ. Policy* **2007**, *9*, 289 – 311.
[238] F. Wei, Y. Liu, W. Z. Qian, G. H. Luo, (Tsinghua Univ) CN 101049927A, **2007**.
[239] a) A. I. Stankiewicz, J. A. Moulijn, *Chem. Eng. Prog.* **2000**, *96*, 22 – 34; b) A. Stankiewicz, J. A. Moulijn, *Ind. Eng. Chem. Res.* **2002**, *41*, 1920 – 1924; c) J. Harmsen, *Chem. Eng. Process.* **2010**, *49*, 70 – 73; d) H. Z. Liu, X. F. Liang, L. R. Yang, J. Y. Chen, *Sci. China Chem.* **2010**, *53*, 1470 – 1475.
[240] T. Van Gerven, A. Stankiewicz, *Ind. Eng. Chem. Res.* **2009**, *48*, 2465 – 2474.
[241] W. C. Ren, F. Li, H. M. Cheng, *J. Phys. Chem. B* **2006**, *110*, 16941 – 16946.
[242] a) Q. F. Liu, W. C. Ren, Z. G. Chen, D. W. Wang, B. L. Liu, B. Yu, F. Li, H. T. Cong, H. M. Cheng, *ACS Nano* **2008**, *2*, 1722 – 1728; b) J. Q. Wei, H. W. Zhu, Y. Jia, Q. K. Shu, C. G. Li, K. L. Wang, B. Q. Wei, Y. Q. Zhu, Z. C. Wang, J. B. Luo, W. J. Liu, D. H. Wu, *Carbon* **2007**, *45*, 2152 – 2158; c) T. X. Cui, R. T. Lv, Z. H. Huang, M. X. Wang, F. Y. Kang, K. L. Wang, D. H. Wu, *Mater. Lett.* **2011**, *65*, 587 – 590.
[243] a) Y. L. Li, I. A. Kinloch, A. H. Windle, *Science* **2004**, *304*, 276 – 278; b) X. H. Zhong, Y. L. Li, Y. K. Liu, X. H. Qiao, Y. Feng, J. Liang, J. Jin, L. Zhu, F. Hou, J. Y. Li, *Adv. Mater.* **2010**, *22*, 692 – 696.
[244] a) P. B. Amama, C. L. Pint, L. McJilton, S. M. Kim, E. A. Stach, P. T. Murray, R. H. Hauge, B. Maruyama, *Nano Lett.* **2009**, *9*, 44 – 49; b) J. X. Liu, Z. Ren, L. Y. Duan, Y. C. Xie, *Acta Chim. Sin.* **2004**, *62*, 775 – 782; c) Z. B. Zhao, J. Y. Qu, J. S. Qiu, X. Z. Wang, Z. Y. Wang, *Chem. Commun.* **2006**, 594 – 596.
[245] T. Yamada, A. Maigne, M. Yudasaka, K. Mizuno, D. N. Futaba, M. Yumura, S. Iijima, K. Hata, *Nano Lett.* **2008**, *8*, 4288 – 4292.
[246] a) Z. R. Li, Y. Xu, X. D. Ma, E. Dervishi, V. Saini, A. R. Biris, D. Lupu, A. S. Biris, *Chem. Commun.* **2008**, 3260 – 3262; b) J. Qu, Z. Zhao, Z. Wang, X. Wang, J. Qiu, *Carbon* **2010**, *48*, 1465 – 1472.
[247] J. Q. Huang, Q. Zhang, M. Q. Zhao, F. Wei, *Nano Res.* **2009**, *2*, 872 – 881.
[248] a) Q. Wen, W. Z. Qian, F. Wei, G. Q. Ning, *Nanotechnology* **2007**, *18*, 215610; b) X. S. Li, X. F. Zhang, L. J. Ci, R. Shah, C. Wolfe, S. Kar, S. Talapatra, P. M. Ajayan, *Nanotechnology* **2008**, *19*, 455609.
[249] D. N. Futaba, J. Goto, S. Yasuda, T. Yamada, M. Yumura, K. Hata, *Adv. Mater.* **2009**, *21*, 4811 – 4815.
[250] H. Yu, Z. F. Li, G. H. Luo, F. Wei, *Diamond Relat. Mater.* **2006**, *15*, 1447 – 1451.

[251] D. C. Wei, Y. Q. Liu, L. C. Cao, L. Fu, X. L. Li, Y. Wang, G. Yu, *J. Am. Chem. Soc.* **2007**, *129*, 7364 – 7368.
[252] D. C. Wei, Y. Q. Liu, L. C. Cao, L. Fu, X. L. Li, Y. Wang, G. Yu, D. B. Zhu, *Nano Lett.* **2006**, *6*, 186 – 192.
[253] D. C. Wei, Y. Q. Liu, *Adv. Mater.* **2008**, *20*, 2815 – 2841.
[254] R. Lv, L. Zou, X. Gui, F. Kang, Y. Zhu, H. Zhu, J. Wei, J. Gu, K. Wang, D. Wu, *Chem. Commun.* **2008**, 2046 – 2048.
[255] a) Z. Chen, D. Higgins, Z. W. Chen, *Carbon* **2010**, *48*, 3057 – 3065; b) E. Y. Xu, J. Q. Wei, K. L. Wang, Z. Li, X. C. Gui, Y. Jia, H. W. Zhu, D. H. Wu, *Carbon* **2010**, *48*, 3097 – 3102; c) T. X. Cui, R. T. Lv, F. Y. Kang, Q. Hu, J. L. Gu, K. L. Wang, D. H. Wu, *Nanoscale Res. Lett.* **2010**, *5*, 941 – 948; d) P. Ayala, R. Arenal, M. Rummeli, A. Rubio, T. Pichler, *Carbon* **2010**, *48*, 575 – 586; e) B. Wang, Y. F. Ma, Y. P. Wu, N. Li, Y. Huang, Y. S. Chen, *Carbon* **2009**, *47*, 2112 – 2115; f) C. P. Ewels, M. Glerup, *J. Nanosci. Nanotechnol.* **2005**, *5*, 1345 – 1363; g) R. T. Lv, T. X. Cui, M. S. Jun, Q. Zhang, A. Y. Cao, D. S. Su, Z. J. Zhang, S. H. Yoon, J. Miyawaki, I. Mochida, F. Y. Kang, *Adv. Funct. Mater.* **2011**, *21*, 999 – 1006; h) S. S. Yu, W. T. Zheng, *Nanoscale* **2010**, *2*, 1069 – 1082.
[256] J. Zhang, X. Liu, R. Blume, A. H. Zhang, R. Schlogl, D. S. Su, *Science* **2008**, *322*, 73 – 77.
[257] B. Frank, J. Zhang, R. Blume, R. Schlogl, D. S. Su, *Angew. Chem.* **2009**, *121*, 7046 – 7051; *Angew. Chem. Int. Ed.* **2009**, *48*, 6913 – 6917.
[258] D. S. Su, *ChemSusChem* **2009**, *2*, 1009 – 1020, and references therein.
[259] M. Endo, K. Takeuchi, Y. A. Kim, K. C. Park, T. Ichiki, T. Hayashi, T. Fukuyo, S. Linou, D. S. Su, M. Terrones, M. S. Dresselhaus, *ChemSusChem* **2008**, *1*, 820 – 822.
[260] M. Q. Zhao, Q. Zhang, J. Q. Huang, J. Q. Nie, F. Wei, *ChemSusChem* **2010**, *3*, 453 – 459.
[261] a) D. Gournis, M. A. Karakassides, T. Bakas, N. Boukos, D. Petridis, *Carbon* **2002**, *40*, 2641 – 2646; b) W. D. Zhang, I. Y. Phang, T. X. Liu, *Adv. Mater.* **2006**, *18*, 73 – 77.
[262] J. Q. Nie, Q. Zhang, M. Q. Zhao, J. Q. Huang, Q. A. Wen, Y. Cui, W. Z. Qian, F. Wei, *Carbon* **2011**, *49*, 1568 – 1580.
[263] A. Rinaldi, N. Abdullah, M. Ali, A. Furche, S. B. A. Hamid, D. S. Su, R. Schlogl, *Carbon* **2009**, *47*, 3023 – 3033.
[264] J. G. Zhao, X. Y. Guo, Q. Q. Guo, L. Gu, Y. Guo, F. Feng, *Carbon* **2011**, *49*, 2155 – 2158.
[265] O. M. Dunens, K. J. MacKenzie, A. T. Harris, *Carbon* **2010**, *48*, 2375 – 2377.
[266] O. M. Dunens, K. J. MacKenzie, A. T. Harris, *Environ. Sci. Technol.* **2009**, *43*, 7889 – 7894.
[267] a) J. S. Qiu, Y. F. Li, Y. P. Wang, T. H. Wang, Z. B. Zhao, Y. Zhou, F. Li, H. M. Cheng, *Carbon* **2003**, *41*, 2170 – 2173; b) J. S. Qiu, Z. Y. Wang, Z. B. Zhao, T. H. Wang, *Fuel* **2007**, *86*, 282 – 286; c) X. F. Zhao, J. S. Qiu, Y. X. Sun, C. Hao, T. J. Sun, L. W. Cui, *New Carbon Mater.* **2009**, *24*, 109 – 113.
[268] R. Bonadiman, M. D. Lima, M. J. de Andrade, C. P. Bergmann, *J. Mater. Sci.* **2006**, *41*, 7288 – 7295.
[269] a) J. Q. Huang, Q. Zhang, F. Wei, W. Z. Qian, D. Z. Wang, L. Hu, *Carbon* **2008**, *46*, 291 – 296; b) W. Z. Qian, H. Yu, F. Wei, Q. F. Zhang, Z. W. Wang, *Carbon* **2002**, *40*, 2968 – 2970; c) Q. Zhang, Y. Liu, J. Q. Huang, W. Z. Qian, Y. Wang, F. Wei, *Nano* **2008**, *3*, 95 – 100; d) P. Ndungu, Z. G. Godongwana, L. F. Petrik, A. Nechaev, S. Liao, V. Linkov, *Microporous Mesoporous Mater.* **2008**, *116*, 593 – 600; e) J. M. Zhou, G. D. Lin, H. B. Zhang, *Catal. Commun.* **2009**, *10*, 1944 – 1947.
[270] P. Ghosh, R. A. Afre, T. Soga, T. Jimbo, *Mater. Lett.* **2007**, *61*, 3768 – 3770.
[271] R. A. Afre, T. Soga, T. Jimbo, M. Kumar, Y. Ando, M. Sharon, *Chem. Phys. Lett.* **2005**, *414*, 6 – 10.
[272] a) M. Kumar, Y. Ando, *J. Nanosci. Nanotechnol.* **2010**, *10*, 3739 – 3758; b) M. Kumar, T. Okazaki, M. Hiramatsu, Y. Ando, *Carbon* **2007**, *45*, 1899 – 1904; c) M. Kumar, Y. Ando, *Carbon* **2005**, *43*, 533 – 540.
[273] X. G. Liu, Y. Z. Yang, H. Y. Liu, W. Y. Ji, C. Y. Zhang, B. S. Xu, *Mater. Lett.* **2007**, *61*, 3916 – 3919.
[274] Z. H. Kang, E. B. Wang, B. D. Mao, Z. M. Su, L. Chen, L. Xu, *Nanotechnology* **2005**, *16*, 1192 – 1195.
[275] A. Meier, V. A. Kirillov, G. G. Kuvshinov, Y. I. Mogilnykh, A. Reller, A. Steinfeld, A. Weidenkaff, *Chem. Eng. Sci.* **1999**, *54*, 3341 – 3348.
[276] W. H. Qian, T. Liu, Z. W. Wang, F. Wei, Z. F. Li, G. H. Luo, Y. D. Li, *Appl. Catal. A* **2004**, *260*, 223 – 228.
[277] W. Z. Qian, T. Tian, C. Y. Guo, Q. Wen, K. J. Li, H. B. Zhang, H. B. Shi, D. Z. Wang, Y. Liu, Q. Zhang, Y. X. Zhang, F. Wei, Z. W. Wang, X. D. Li, Y. D. Li, *J. Phys. Chem. C* **2008**, *112*, 7588 – 7593.
[278] a) Y. D. Li, J. L. Chen, Y. N. Qin, L. Chang, *Energy Fuels* **2000**, *14*, 1188 – 1194; b) D. X. Li, J. L. Chen, Y. D. Li, *Int. J. Hydrogen Energy* **2009**, *34*, 299 – 307; c) Y. D. Li, D. X. Li, G. W. Wang, *Catal. Today* **2011**, *162*, 1 – 48.
[279] W. Z. Qian, T. Liu, F. Wei, Z. W. Wang, Y. D. Li, *Appl. Catal. A* **2004**, *258*, 121 – 124.
[280] J. Q. Huang, Q. Zhang, M. Q. Zhao, F. Wei, *Carbon* **2010**, *48*, 1441 – 1450.
[281] C. N. He, N. Q. Zhao, C. S. Shi, X. W. Du, J. J. Li, H. P. Li, Q. R. Cui, *Adv. Mater.* **2007**, *19*, 1128 – 1132.
[282] a) H. P. Li, N. Q. Zhao, Y. Liu, C. Y. Liang, C. S. Shi, X. W. Du, J. J. Li, *Composites Part A* **2008**, *39*, 1128 – 1132; b) A. K. Keshri, J. Huang, V. Singh, W. B. Choi, S. Seal, A. Agarwal, *Carbon* **2010**, *48*, 431 – 442; c) A. Peigney, F. L. Garcia, C. Estournes, A. Weibel, C. Laurent, *Carbon* **2010**, *48*, 1952 – 1960.
[283] a) L. J. Ci, Z. G. Zhao, J. B. Bai, *Carbon* **2005**, *43*, 883 – 886; b) Z. G. Zhao, L. J. Ci, H. M. Cheng, J. B. Bai, *Carbon* **2005**, *43*, 663 – 665; c) J. O. Zhao, L. Liu, Q. G. Guo, J. L. Shi, G. T. Zhai, J. R. Song, Z. J. Liu, *Carbon* **2008**, *46*, 380 – 383.
[284] H. Zhang, G. P. Cao, Z. Y. Wang, Y. S. Yang, Z. N. Gu, *Carbon* **2008**, *46*, 822 – 824.
[285] G. Li, S. Chakrabarti, M. Schulz, V. Shanov, *J. Mater. Res.* **2009**, *24*, 2813 – 2820.
[286] Q. Wen, T. Tian, W. Z. Qian, L. Hu, S. Yun, A. Y. Cao, F. Wei, *J. Electrochem. Soc.* **2008**, *155*, K180 – K182.
[287] a) S. Talapatra, S. Kar, S. K. Pal, R. Vajtai, L. Ci, P. Victor, M. M. Shaijumon, S. Kaur, O. Nalamasu, P. M. Ajayan, *Nat. Nanotechnol.* **2006**, *1*, 112 – 116; b) L. J. Gao, A. P. Peng, Z. Y. Wang, H. Zhang, Z. J. Shi, Z. N. Gu, G. P. Cao, B. Z. Ding, *Solid State Commun.* **2008**, *146*, 380 – 383; c) S. K. Pal, S. Kar, S. Lastella, A. Kumar, R. Vajtai, S. Talapatra, T. Borca-Tasciuc, P. M. Ajayan, *Carbon* **2010**, *48*, 844 – 853.
[288] a) H. L. Zhang, Y. Zhang, X. G. Zhang, F. Li, C. Liu, J. Tan, H. M. Cheng, *Carbon* **2006**, *44*, 2778 – 2784; b) X. L. Li, S. H. Yoon, K. Du, Y. X. Zhang, J. M. Huang, F. Y. Kang, *Electrochim. Acta* **2010**, *55*, 5519 – 5522.
[289] H. Zhang, G. P. Cao, Y. S. Yang, *Energy Environ. Sci.* **2009**, *2*, 932 – 943.
[290] X. S. Li, G. Y. Zhu, J. S. Dordick, P. M. Ajayan, *Small* **2007**, *3*, 595 – 599.
[291] Y. Liu, W. Z. Qian, Q. Zhang, A. Y. Cao, Z. F. Li, W. P. Zhou, Y. Ma, F. Wei, *Nano Lett.* **2008**, *8*, 1323 – 1327.
[292] K. Kordas, G. Toth, P. Moilanen, M. Kumpumaki, J. Vahakangas, A. Uusimaki, R. Vajtai, P. M. Ajayan, *Appl. Phys. Lett.* **2007**, *90*, 123 105.
[293] M. Bozlar, D. L. He, J. B. Bai, Y. Chalopin, N. Mingo, S. Volz, *Adv. Mater.* **2010**, *22*, 1654 – 1658.
[294] L. Song, L. Ci, L. Lv, Z. P. Zhou, X. Q. Yan, D. F. Liu, H. J. Yuan, Y. Gao, J. X. Wang, L. F. Liu, X. W. Zhao, Z. X. Zhang, X. Y. Dou, W. Y. Zhou, G. Wang, C. Y. Wang, S. S. Xie, *Adv. Mater.* **2004**, *16*, 1529 – 1534.
[295] Q. F. Liu, W. C. Ren, D. W. Wang, Z. G. Chen, S. F. Pei, B. L. Liu, F. Li, H. T. Cong, C. Liu, H. M. Cheng, *ACS Nano* **2009**, *3*, 707 – 713.
[296] a) K. L. Jiang, Q. Q. Li, S. S. Fan, *Nature* **2002**, *419*, 801 – 801; b) Q. W. Li, X. F. Zhang, R. F. DePaula, L. X. Zheng, Y. H. Zhao, L. Stan, T. G. Holesinger, P. N. Arendt, D. E. Peterson, Y. T. Zhu, *Adv. Mater.* **2006**, *18*, 3160 – 3165; c) M. Zhang, S. L. Fang, A. A. Zakhidov, S. B. Lee, A. E. Aliev, C. D. Williams, K. R. Atkinson, R. H. Baughman, *Science* **2005**, *309*, 1215 – 1219; d) M. Musameh, M. R. Notivoli, M. Hickey, I. L. Kyratzis, Y. A. Gao, C. Huynh, S. C. Hawkins, *Adv. Mater.* **2011**, *23*, 906 – 910; e) M. D. Lima, S. L. Fang, X. Lepro, C. Lewis, R. Ovalle-Robles, J. Carretero-Gonzalez, E. Castillo-Martinez, M. E. Kozlov, J. Y. Oh, N. Rawat, C. S. Haines, M. H. Haque, V. Aare, S. Stoughton, A. A. Zakhidov, R. H. Baughman, *Science* **2011**, *331*; f) Q. Zhang, D. G. Wang, J. Q. Huang, W. P. Zhou, G. H. Luo, W. Z. Qian, F. Wei, *Carbon* **2010**, *48*, 2855 – 2861; g) H. S. Jang, S. K. Jeon, S. H. Nahm, *Carbon* **2011**, *49*, 111 – 116; h) M. H. Miao, J. McDonnell, L. Vuckovic, S. C. Hawkins, *Carbon* **2010**, *48*, 2802 – 2811; i) K. L. Jiang, J. P. Wang, Q. Q. Li, L. Liu, C. H. Liu, S. S. Fan, *Adv. Mater.* **2011**, *23*, 1154 – 1161.
[297] Y. Ando, X. Zhao, K. Hirahara, K. Suenaga, S. Bandow, S. Iijima, *Chem. Phys. Lett.* **2000**, *323*, 580 – 585.
[298] X. Lv, F. Du, Y. F. Ma, Q. Wu, Y. S. Chen, *Carbon* **2005**, *43*, 2020 – 2022.

Received: April 5, 2011

